NETWORK CONVERGENCE IN MULTICARRIER HYBRID CELLULAR NETWORK

A Dissertation
Submitted to the Graduate Faculty
of the
North Dakota State University
of Agriculture and Applied Science

By

Siqian Liu

In Partial Fulfillment
for the Degree of
DOCTOR OF PHILOSOPHY

Major Department:
Electrical and Computer Engineering

July 2014

Fargo, North Dakota

North Dakota State University
Graduate School

Title

Network Convergence in Multicarrier Hybrid Cellular Network

By

Siqian Liu

The Supervisory Committee certifies that this ***disquisition*** complies with North Dakota State University's regulations and meets the accepted standards for the degree of

DOCTOR OF PHILOSOPHY

SUPERVISORY COMMITTEE:

Hongxiang Li
Co-Chair

Benjamin D. Braaten
Co-Chair

Rajesh Kavasseri

Jason Boynton

Approved:

July.11th.2014
Date

Scott C. Smith
Department Chair

ABSTRACT

In a multicarrier communication system with known channel state information at transmitter (CSIT), it is well-known that the water-filling power allocation scheme is optimal in achieving the Shannon capacity. However, in a multicarrier broadcast network (e.g. over-the-air TV network) without CSIT, the optimal power allocation among subcarriers is still unknown, largely due to the heterogeneity of the channel conditions associated with different receivers. In the first part of the thesis, the performance of a generic multicarrier broadcast network is thoroughly studied by exploiting the frequency diversity over subcarriers. In particular, the performance metric is first defined based on the relationship among broadcast transmission rate, coverage area and outage probability. In order to maximize the network performance, closed form expressions of the instantaneous mutual information (IMI) and the optimal power allocation schemes are derived for both low SNR and high SNR cases; upper and lower bounds are also provided to estimate broadcast coverage area in general SNR regime. Also we extend our discussion to the broadcast network with multiple collaborative transmitters. Extensive simulation results are provided to validate our analysis.

In the second part of the thesis, we discuss the optimal performance of a generic broadcast cellular hybrid network. It is well known that the Dirty Paper Coding (DPC) achieves the channel capacity for multiuser degraded channels. However, the optimality of DPC remains unknown for non-degraded channel. Specifically, we derive the optimal interference pre-cancellation order for a DPC based broadcast and unicast hybrid network. Different DPC cancellation schemes are studied to maximize the hybrid capacity region. The conditions for each scheme being optimal are analytically derived. Both ergodic and outage capacity are considered as our performance metric. Our results show that the optimal interference pre-cancellation order varies with SNR

and broadcast and unicast channel conditions. Moreover, in low SNR condition, the optimal power allocation scheme is derived to reach the maximal sum rate.

ACKNOWLEDGMENTS

First of all, I would like to thank my advisor, Professor Hongxiang Li, for his consistent support and invaluable guidance during my Ph.D study. I am very grateful for the opportunities he provided to me so that I can keep studying and pursue my interests in the past five years. The inspiration and recognition received from him will be deeply cultivated in my future life and work.

Secondly, I want to thank Professor Benjamin Braaten, Professor Gou Bei, Professor Rajesh Kavasseri and Professor Jason Boynton for their effort and time spent on my dissertation work. They provide many precious advice and useful comments during the development of this dissertation.

I also wish to express my thanks to all my classmates, including Dr. Tuan Tran, Guanying Ru, Claudia Sampaio, Varinder Singh and Dr Yang Du for a lot of collaboration and discussion we had. The friendship with them becomes a joyful and indispensable part during my pursuit of degree.

Finally, I would like to thank my parents for their support and understanding during my study to pursue this work.

TABLE OF CONTENTS

LIST OF TABLES

LIST OF FIGURES

LIST OF SYMBOLS

M ..... Total number of broadcast signal

K ..... Total number of unicast signal

$h_i^b(j)$ .....Subcarrier channel gain of ith broadcast signal on subcarrierr j

$h_i^u(j)$ .....Subcarrier channel gain of ith unicat signal on subcarrierr j

P ..... Total transmitting power

$P_i^b(j)$ .....Power allocated to ith broadcast signal on subcarrierr j

$P_i^u(j)$ .....Power allocated to ith unicast signal on subcarrierr j

N_r ..... Number of antennas at transmitter

N_T ..... Number of antenna at receiver

B ..... Total system bandwidth

B_n ..... Subchannel bandwidth

C_{hybrid} ..... Capacity region of hybrid network

q^0 ..... Outage probability

$\underset{x}{max}\{f(x)\}$ ..... Maximum value of $f(x)$ maximized over all x

LIST OF APPENDIX FIGURES

Figure Page

CHAPTER 1. INTRODUCTION

In the past decades, the progress of wireless communication has substantially changed the way we live and lead to the prosperity of today's smartphone market. People nowadays are able to get connected to internet through wireless local area network (WLAN) or cellular network almost everywhere. Many of household appliances, for example TV, refrigerator, air condition and coffee machine, are starting to get connected through wireless network to facilitate our daily life. Moreover, the upcoming wearable devices such as smart watch and google glass, will even get our body connected to internet through wireless technology.

With all these applications, wireless network is facing lots of challenges to meet the explosive increasing demand on performance. Many breakthrough innovative technologies in wireless communication have been implemented to greatly enhance the network performance: CDMA, OFDM, MIMO and dirty-paper precoding.

1.1. Motivation

Wireless communities across the countries are facing the same serious challenge: the severe spectrum shortage along with explosive increase in the number of mobile devices and real time multimedia applications. Within allowed frequency band (e.g.: 2.4GHz, 5GHz), more users needs to be accommodated at the same time carrying different information. In order to better fulfill the service requirement for more users as possible, we need to reasonably design the multiplexing scheme for the system and optimally allocate available resource (e.g.: power, bandwidth, time slots). Recent years,multicarrier transmission/orthogonal frequency division multiplexing (OFDM) has become the main technology used in wireless system due to its easy implementation and robustness to fading and interference. Many standards and broadband networks (e.g.: IEEE 802.11a/g/n/ac WLAN, IEEE 802.16 WiMax, 4G-LTE) have adopt it as the solution to push for the performance limit of the network.

However, previous studies are mainly based on symmetric communication model with both uplink and downlink, the performance of multicarrier transmission in non-symmetric communication scenario such as broadcast network has not been thoroughly studied.

On the other hand, due to the scarcity of the spectrum resource, many wireless applications are overlapping in spectrum and interfering each other. For example, WLAN, Bluetooth and LTE band-40 are operating on or close to 2.4GHz ISM band. Hence, proper wireless coexistence schemes are implemented to avoid/mitigate interference. Traditionally, time division multiplexing (TDM), frequency hopping(FH) and cognitive radio are used to accommodate different application signal and utilize the spectrum more efficiently. However, the achievable rate are still far below the theoretical channel capacity due to their non-collaborative nature.

Throughout our discussion, we classify the wireless signal into two types: broadcast and unicast. We define broadcast (BC) as the distribution of common information (such as TV program) over unidirectional channels (one-way communication) to many receivers; and unicast (UC) is referred to symmetric applications such as voice telephony and data access where the transmitter exchanges private information with individual receiver over bi-directional channels (two-way communications). In unicast, we assume the instantaneous channel state information (CSI) is available at the transmitter, which can be achieved through channel reciprocity in time-division duplex (TDD) systems and uplink channel feedback in frequency-division duplex (FDD) systems. For broadcast, without receiver feedback, it is reasonable to assume only the channel statistics are available at the transmitter [1]-[3].

1.1.1. Multicarrier broadcast system

In mobile broadband communication, one of the major problem is the performance impairment brought by inter-symbol interference (ISI). ISI mainly occurs when

system's bandwidth is larger than coherence bandwidth which is pre-determined by environment (multipath effect). In order to reduce the effect of ISI while maintaining system's performance, multicarrier transmission has been proposed for wireless network. The basic idea of multicarrier transmission is to divide the whole data stream into several segments and modulate them on some parallel narrowband subchannels. Since rate on each of the subchannels is much less than the original data rate, the bandwidth of each subchannel is much smaller than the original system bandwidth. In this way, we transform a broadband communication system to a narrowband system consisting of several subchannels. Each subchannel's bandwidth is smaller than bandwidth thus it experiences slow-fading during transmission.

Since the start of European Digital Audio Broadcasting (E-DAB) and Digital Video Broadcasting (DVB) projects in 1980s, the debate on multicarrier transmission versus single-carrier transmission has never stopped [9]. Conventionally, single-carrier transmission has been widely studied in broadcast network [10, 11, 12, 13] and adopted by some digital terrestrial broadcast standards (e.g. ATSC, DTMB) [14, 15]. Compared to single-carrier transmission, multicarrier transmission can deliver broadband data without using complicated time-domain equalizer. Due to its simplicity and easy implementation, multicarrier transmission has been adopted by many digital video broadcasting standards such as DVB and ISDB [17].

1.1.2. Broadcast and unicast hybrid network

Nowadays, the communication industry is experiencing a fast growing in number of users. The demand of various services also keeps increasing in an unprecedented speed. Even though the current 3G/4G network is much more powerful than the traditional GPRS and GSM, there are still many limitations such as the transmission of large files or the support of the large data throughput. In wireless network, more and more service providers are required to offer the broadcasting TV (e.g.: DVB) and

the broadband internet connection (e.g.: WiMAX) simultaneously. However, these two types of connection are different to each other due to their inherent differences in network structure and communication strategy. Moreover, with the prevalence of the multi-resolution TV, users may have different needs for the quality to the TV services, such as High-definition TV (HDTV) and Standard-definition (SDTV). The schemes and requirements in the transmission these TV signals are also varied. In some country such as Japan, research on offering HDTV through mobile network is in progress and some results have been obtained. At the same time, since the broadcast communication has developed more than 100 years, by now with the application of the appropriate coding schemes, it is very close to the Shannon capacity which is the maximum transmission rate can be achieved.

In order to overcome these challenges, cellular hybrid networks become an intriguing concept since it can incorporate the broadcast and cellular communications with the same infrastructure. A common platform can be built to collaboratively transmit both broadcast and cellular signals. Such cooperation is also the natural path of evolution of the wireless communication and expected to enhance the performance of both networks significantly. Even though there are some service-providers such as Verizon and Sprint are staring to offer the mobile TV services through the current cellular network, both the number and the quality of the programs are quite limited by the network. The hybrid network can easily solve such problems due to its infrastructure. Furthermore, such cooperation can greatly reduce both cost of building the individual broadcast and cellular base stations and the maintenance fees.

While the hybrid network posses so much advantages, it is still unclear the optimal transmission schemes in it. In this thesis, our goal is to jointly design and optimize both networks by investigating some fundamental architectural changes to achieve the true potential of a collaborative cellular network.

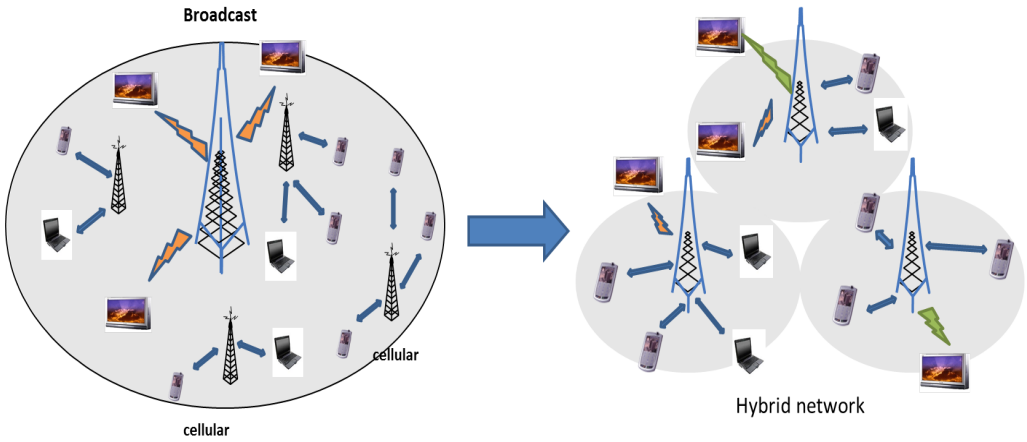

Figure 1.1. Convergence of different networks

1.2. Outline

This dissertation is organized as follow: In Chapter 2, we first define the performance metric and system model for generic multicarrier broadcast networks. We present performance analysis of single transmitter multicarrier broadcast network is provided, along with the optimal power allocation schemes that maximize the network coverage. Then we extend the results to multi-transmitter broadcast network. Our primary goal is to find out the optimal resource allocation scheme and numerical approximation to compute broadcast coverage in both high SNR and low SNR condition.

In Chapter 3, we investigate the optimal DPC-cancellation order in a general hybrid network. We first give a brief description of the general hybrid system model. Then, the optimal DPC interference pre-cancellation order for only one broadcast signal and one unicast signal is analytically derived. Based on that, results are extended to a general hybrid network framework with multicarrier transmission. We also derive the optimal power allocation scheme in low SNR condition to maximize the overall network performance. Future research topics are discussed in Chapter 4.

Finally, as another significant research work during my Ph.D study, some research results about power line communication channel modeling are presented. Since this part of work is independent to the thesis topic, we put it in appendix for reference.

CHAPTER 2. MULTICARRIER BROADCAST NETWORK ANALYSIS

The conventional broadcast industry is experiencing a growing diffusion of new services. Worldwide, the old analog broadcast TV is being replaced by digital broadcast TV to improve the quality of service (QoS) and better utilize existing TV spectrum. On the other hand, with the prevalence of mobile devices such as smart phones and tablets, the demand for mobile wireless multimedia services keeps increasing at an unprecedented speed [4]. In particular, major wireless providers have started offering mobile TV services in many parts of the world. According to [5], the number of mobile TV subscribers worldwide has grown at a compound annual rate of over 47% since 2010 and reached 570 Million by the end of 2013. Note that, unlike the broadcast TV network, existing mobile TV services are largely offered in unicast fashion. Here, *unicast* is defined as the delivery of private information to individual user with point-to-point connection (e.g. video on demand). Due to the increasing demand for wireless multimedia services and the scarcity of radio spectrum, the unfavorable scaling behavior of unicast can become a serious issue: the network resources will be quickly depleted when there are many users watching TV at the same time [6]. Apparently, for high demand multimedia services, broadcast is more resource (energy and spectrum) efficient since a single transmission will accommodate all users simultaneously. In the literature, the term "broadcast" has been used for both TV/radio services and mobile cellular downlink channels. To avoid ambiguity, in this paper we define *broadcast* as the delivery of the same common information (e.g. TV program) to all receivers. To provide capacity offload from unicast transmissions, the Multimedia Broadcast/Multicast Service (MBMS) was introduced in 3GPP LTE [7]. In US, Verizon is the first wireless operator to announce that it will launch evolved MBMS services in 2014, over its LTE networks [8]. Despite

these developments, the fundamental limits of broadcast transmission have not been thoroughly studied compared with its unicast counterpart. This part will focus on fundamental performance analysis of broadcast technologies that are applicable to both the terrestrial TV network and the mobile cellular network.[1]

Since the start of European Digital Audio Broadcasting (E-DAB) and Digital Video Broadcasting (DVB) projects in 1980s, the debates on multicarrier transmission versus single-carrier transmission have never stopped [9]. Conventionally, single-carrier transmission has been widely studied in broadcast network [10, 11, 12, 13] and adopted by some digital terrestrial broadcast standards (e.g. ATSC, DTMB) [14, 15]. In ATSC, single-carrier trellis-coded 8-level vestigial side-band (TC-8VSB) modulation is used to transfer multimedia data at a maximum rate of 19.39 Mbps [16]. Compared with single-carrier transmission, multicarrier transmission divides the total system bandwidth into parallel subcarriers, which effectively mitigates the frequency-selectivity of the channel and delivers broadband data without complicated time-domain equalization. Due to its simplicity and easy implementation, multicarrier transmission (e.g. OFDM) has been adopted by many digital video broadcasting standards such as DVB in Europe and ISDB in Japan [17]. In DVB-T, using COFDM and 64-QAM, the maximum data rate can reach 31.2 Mbps [18, 19]. In ISDB-T, the so called Bandwidth Segmented Transmission OFDM (BST-OFDM) is applied to support both HDTV and SDTV service in high-speed moving vehicle at the maximum data rate of 23 Mbps [20, 21].

In multicarrier broadcast networks (MBN), channel coding can be applied either independently on each subcarrier (in short as *independent coding*) or jointly over all subcarriers (in short as *joint coding*) [22]. While independent coding is easier to implement, it decreases the achievable transmission rate in MBN comparing with

[1]This part of work has been submitted to IEEE Transaction for publication

joint-coding [23]. Notably, our previous study [24] found out that independent coding cannot fully exploit the frequency diversity among subcarriers and yields poor outage performance in a broadcast and unicast hybrid wireless network. In joint coding, information is encoded and decoded over all subcarriers jointly so that the transmission outage probability is minimized under the same coding rate [25, 26]. Therefore, the joint coding has been adopted by many multicarrier transmission systems (DVB-H, WLAN, etc.) [27, 28, 29]. However, to the best of our knowledge, there is no detailed and rigorous performance analysis of MBN with joint coding. The main contribution of this part is to analyze the MBN performance with joint coding from an information theoretic point of view.

Moreover, we extend our results of single transmitter MBN [30] to a broadcast network with multiple transmitters. In this case, there are two types of transmission schemes in existing broadcast systems: the traditional multi-frequency network (MFN) and the new single frequency network (SFN) [31]. In MFN, multiple transmitters broadcast on different frequencies to avoid interference. In SFN, multiple transmitters send the same signal over the same frequency channel at the same time. With the added spatial diversity, SFN offers advantages in terms of the received signal strength [32, 33]. However, it does not fully exploit the multiple antenna gain [34]. To further improve the performance, the multi-cell cooperation (MCC, a.k.a. distributed antenna system) has been studied in cellular unicast network to prescribe the signals from multiple base stations (BSs), which are inter-connected via high capacity backbone [35, 36]. Similarly in MBN, multiple broadcast-station cooperation (MBC) is expected to have better performance compared with SFN because it can further exploit the spatial diversity [37]. To the best of our knowledge, despite many existing studies on SFN and MBC [38, 39, 40], their performance in jointly coded MBN has not been studied.

2.1. Multicarrier broadcast system model

2.1.1. Performance metric

In a multicarrier unicast system (e.g. cellular network) with known channel state information at transmitter (CSIT), it is well-known that the water-filling power allocation scheme is optimal in achieving the Shannon capacity [41, 42, 43, 44, 45, 46]. However, in the traditional broadcast TV network, CSIT is not available due to the lack of reverse link. For broadcast/multicast services over cellular network, even though CSIT is possible via channel feedback, the transmitter cannot optimize its transmission based on an individual receiver's CSI due to the heterogeneity of channel conditions associated with different receivers. Therefore, we consider a MBN where the transmitter only knows the channel distribution information (CDI) in a given service area. In this case, there are two channel capacity definitions that are relevant to the broadcast system design: *ergodic capacity* and *outage capacity* [47]. In practice, ergodic capacity only applies to fast fading channels and the capacity-achieving code must be sufficiently long so that a received codeword is affected by all possible fading states, which will cause significant delay and thus is not suitable for practical broadcast applications. Alternatively, outage capacity can deal with slow fading channels by defining the maximum data transmission rate that the received data are decoded with certain outage probability. That is to say, if the received signal to interference and noise ratio (SINR) is above the threshold corresponding to the outage probability, the transmitted data can be decoded correctly. Otherwise, the reception is in outage. By allowing the receiver to lose some data in the event of slow deep fading, the received data can be decoded instantly to meet the broadcast delay requirement. In this part, we consider a generic broadcast network with slow fading channels[1] and choose outage capacity as the figure of merit for performance

[1]The assumption of slow fading channels is applicable to both broadcast TV networks with stationary receivers and mobile cellular network with slow moving receivers.

evaluation. Note that outage capacity is also the performance metric for current digital TV standards (DVB-N/G/H, ATSC-M/H and etc.) [48, 49] and some related studies can be found in [50, 51, 52].

In broadcast applications, receivers at different geographic locations decode the same broadcast signal with different outage probabilities based on their heterogeneous channel conditions. For simplicity, we consider a two-dimensional broadcast service area A without shadowing, i.e., the variation in received signal power is determined by free-space path loss and multipath fading. Due to the heterogeneity of broadcast channels, the broadcast network shall guarantee a minimum QoS to all users. That is, within the service area A, the outage probability of any receiver should be upper-bounded by a predetermined probability q_0. If we denote w as a user on the boundary of A who has the worst channel statistics and define q^w as the outage probability associated with this user, the broadcast network QoS requirement can be expressed as $q^w \leq q_0$. In this way, instead of considering QoS requirements of all users within A, we only need to focus on the performance of user w because any receiver within the service area has an outage probability no higher than q^w.

Let r_0 be the broadcast data transmission rate, there are three alternatives to optimize the broadcast network performance:

1) Given r_0 and q_0, maximize A subject to receiver outage constraint and transmitter power constraint.

2) Given A and q_0, maximize r_0 subject to receiver outage constraint and transmitter power constraint.

3) Given r_0 and A, minimize q_0 subject to receiver outage constraint and transmitter power constraint.

In practical broadcast network, based on the resolution of the multimedia content (e.g. SDTV or HDTV), the data transmission rate of a particular channel is

usually fixed. Meanwhile, the maximum outage probability allowed in a service area is also pre-determined. Therefore, our objective is to maximize the coverage area A. However, it is noteworthy that the above three optimization alternatives are essentially interchangeable: given any two of the three parameters (r_0, q_0, A), optimizing the third one is equivalent to maximizing the instantaneous mutual information (IMI) [26].

2.1.2. Multicarrier broadcast system model

Without loss of generality, we consider a broadcast channel (e.g. TV channel) consisting of N subcarriers of equal bandwidth B_N. To fully exploit frequency diversity, we assume the N subcarriers forming a broadcast channel are sufficiently apart in frequency so that the channel gains are N independent random variables with known distributions, as shown in Figure 2.1. Accordingly, the optimization problem for a single transmitter MBN can be mathematically formulated as:

$$\max_{\overrightarrow{p}=(p_1,p_2,\cdots,p_N)} A \tag{2.1}$$

$$\mathbf{s.t.}: \quad q^w \leq q_0 \tag{2.2}$$

$$q^w = Prob[\overrightarrow{h^w} : I(\overrightarrow{h^w}, \overrightarrow{p}) \leq r_0] \tag{2.3}$$

$$\sum_{n=1}^{N} p_n = P \tag{2.4}$$

where $\overrightarrow{p} = (p_1, p_2, \cdots, p_N)$ is the transmit power vector and $\overrightarrow{h^w} = (h_1^w, h_2^w, \cdots, h_N^w)$ is the channel gain vector associated with user w. In (2.1), our objective is to maximize the coverage area A by finding the optimal power allocation $\overrightarrow{p}$ over N subcarriers. Note that Equation (2.2) and (2.4) are the outage probability constraint and transmit power constraint, respectively.

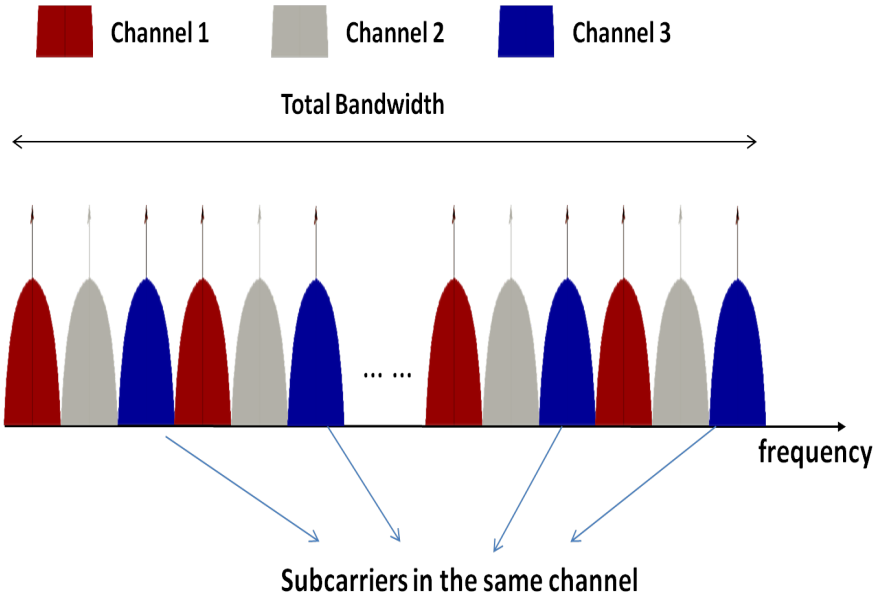

Figure 2.1. Multicarrier transmission in different channels

In particular, Equation (2.3) is the formula for calculating the outage probability with joint-coding, where random variable $I(\overrightarrow{h^w}, \overrightarrow{p})$ is the IMI (also called instantaneous capacity). Apparently, with fixed transmission rate r_0, the outage probability q^w depends solely on the distribution of IMI, which is determined by power allocation vector $\overrightarrow{p}$ and the distributions of $\overrightarrow{h^w}$. Therefore, maximizing the coverage area A is equivalent to optimizing the distribution of $I(\overrightarrow{h^w}, \overrightarrow{p})$ subject to constraints (2.2) and (2.4).

2.2. Multicarrier broadcast coverage in SISO

As we discussed in Section II, the optimization problem boils down to optimize the distribution of IMI. In a MBN with single transmitter, the IMI is given by:

$$I(\overrightarrow{h}, \overrightarrow{p}) = \sum_{n=1}^{N} B_n log_2(1 + \frac{p_n|h_n|^2}{N_0 B_n}) \tag{2.5}$$

$$\textbf{s.t.}: \quad \sum_{n=1}^{N} p_n = P \tag{2.6}$$

where N_0 is the power density of the additive white Gaussian noise (AWGN) and $SNR_n = \frac{p_n|h_n|^2}{N_0 B_n}$ is the signal to noise power radio (SNR) on subcarrier n. It is well know that wireless channel gain is determined by free-space path loss (large-scale propagation effects) and multipath fading (small-scale propagation effects) [47]. According to [26], in broadcast applications, the channel gain $|h|$ is usually assumed to be *Rayleigh* distributed. Therefore, the power gain $|h|^2$ follows $chi - squared$ distribution with mean $E[|h|^2] = 2\sigma^2$, where σ^2 is determined by path loss.

To calculate the broadcast coverage, the probability density function (PDF) of IMI must be known. Unfortunately, getting a closed form expression is difficult because it involves the logarithmic operation and an $n-$fold convolution. In the following analysis, we discuss the distribution of IMI in three different cases depending on SNR.

2.2.1. IMI in general SNR condition

We write IMI as: $I(\overrightarrow{h}, \overrightarrow{p}) = \frac{B_n}{ln2} \sum_{n=1}^{N} B_n ln(1 + \frac{p_n|h_n|^2}{N_0 B_0})$ and denote Y_k as:

$$Y_k = ln(1 + \frac{p_n|h_n|^2}{N_0 B_0}) \tag{2.7}$$

For any given value y_0, the cumulative density function (CDF) of Y_k can be expressed as:

$$F(Y_k \leq y_0) = F[|h_k|^2 \leq \frac{N_0 B_0}{p_k}(e^{y_0} - 1)] \tag{2.8}$$

Taking derivative on both sides, we get the PDF of Y_k:

$$f_{Y_k}(y_0) = \frac{N_0 B_0}{p_k {\sigma_k}^2} e^{\frac{N_0 B_0}{p_k {\sigma_k}^2}} exp[-\frac{N_0 B_0}{p_k {\sigma_k}^2} e^{y_0} + y_0] \tag{2.9}$$

The PDF of IMI can be obtained by doing the convolution:

$$f_I(y) = f_{Y_1}(y) * f_{Y_2}(y) * \cdots f_{Y_N}(y) \tag{2.10}$$

where "*" indicates the convolution operation. For convenience, we denote $\frac{p_k {\sigma_k}^2}{N_0 B_0} = \overline{\sigma_k}^2$, then $f_I(y)$ is given by:

$$f_I(y) = e^{\sum_{k=1}^{N} \frac{1}{\overline{\sigma_k}^2}} (\prod_{k=1}^{N} \frac{1}{\overline{\sigma_k}^2})[exp(y - \frac{e^y}{\overline{\sigma_1}^2}) * \cdots * exp(y - \frac{e^y}{\overline{\sigma_N}^2})] \tag{2.11}$$

When calculating the convolution, the integral $\int exp(Ae^y - Be^{-y})$ has no closed form in general. Fortunately, we can find tight upper and lower bounds for function $f_I(y)$.

Without the loss of generality, we assume $\overline{\sigma_1}^2 \leq \overline{\sigma_2}^2 \leq \cdots \leq \overline{\sigma_N}^2$. The convolution of the first two terms in Equation (2.11) is calculated as:

$$[exp(y - \frac{e^y}{\overline{\sigma_1}^2}) * exp(y - \frac{e^y}{\overline{\sigma_2}^2})] = e^y \int_0^y exp[-(\frac{e^{y-z}}{\overline{\sigma_2}^2} + \frac{e^z}{\overline{\sigma_1}^2})]dz \tag{2.12}$$

Let $k = e^z$, we re-write Equation (2.12) and denote it as $g(y)$:

$$g(y) = e^y \int_1^{e^y} \frac{1}{k} exp[-(\frac{e^y}{\overline{\sigma_2}^2}\frac{1}{k} + \frac{k}{\overline{\sigma_1}^2})]dk \tag{2.13}$$

Because $k \geq 1$, we have the following inequality:

$$\begin{aligned} e^y \int_1^{e^y} \frac{1}{k} exp[-(\frac{e^y}{\overline{\sigma_2}^2} + \frac{k}{\overline{\sigma_1}^2})]dk &\leq g(y) \\ &\leq e^y \int_1^{e^y} \frac{1}{k} exp[-(\frac{e^y}{\overline{\sigma_2}^2}\frac{1}{k} + \frac{1}{\overline{\sigma_1}^2})]dk \end{aligned} \tag{2.14}$$

For the left side of the Equation (2.14):

$$\begin{aligned} e^y \int_1^{e^y} \frac{1}{k} exp[-(\frac{e^y}{\overline{\sigma_2}^2} + \frac{k}{\overline{\sigma_1}^2})]dk \\ = exp(y - \frac{e^y}{\overline{\sigma_2}^2})[\Gamma(0, \frac{1}{\overline{\sigma_1}^2}) - \Gamma(0, \frac{1}{\overline{\sigma_2}^2})] \end{aligned} \tag{2.15}$$

where $\Gamma(s,t) = \int_x^\infty t^{s-1}exp(-t)dt$ is the upper incomplete gamma function. Because $0 \leq y$ and $e^{-y} \leq 1 \leq \frac{\overline{\sigma_2}^2}{\overline{\sigma_1}^2}$, we have:

$$\Gamma(0, \frac{1}{\overline{\sigma_1}^2}) - \Gamma(0, \frac{1}{\overline{\sigma_2}^2}) \leq \Gamma(0, \frac{1}{\overline{\sigma_1}^2}) - \Gamma(0, \frac{e^y}{\overline{\sigma_2}^2}) \tag{2.16}$$

Repeat the above procedures from (2.11) to (2.16) for σ_2^2, σ_3^2 and so on, we can get the lower bound as:

$$exp(y - \frac{e^y}{\overline{\sigma_N}^2}) \prod_{n=1}^{N-1} [\Gamma(0, \frac{1}{\overline{\sigma_n}^2}) - \Gamma(0, \frac{1}{\overline{\sigma_{n+1}}^2})] \tag{2.17}$$

Similarly, the upper bound is calculated as:

$$exp(y - \frac{e^y}{\overline{\sigma_1}^2})[\Gamma(0, \frac{1}{\overline{\sigma_N}^2}) - \Gamma(0, \frac{e^y}{\overline{\sigma_N}^2})] \prod_{n=2}^{N-1} [\Gamma(0, \frac{1}{\overline{\sigma_n}^2}) - \Gamma(0, \frac{1}{\overline{\sigma_{n+1}}^2})] \tag{2.18}$$

For $\Gamma(0,x)$, we can compute it with the following continued fraction:

$$\Gamma(0,x) = \cfrac{e^{-x}}{x + \cfrac{1}{1 + \cfrac{1}{x + \cfrac{2}{1 + \cfrac{2}{x + \cfrac{3}{1 + \cdots}}}}}} \tag{2.19}$$

2.2.2. IMI in low SNR condition

When the SNR on each subcarrier is small, the IMI can be approximated as:

$$I(\overrightarrow{h}, \overrightarrow{p}) = \sum_{n=1}^{N} \frac{1}{ln2} B_n SNR_n = \sum_{n=1}^{N} |h'_n|^2 \tag{2.20}$$

where $|h'_n|^2 = \frac{p_n}{N_0 ln2}|h_n|^2$ is still chi-squared distributed with $E[|h'_n|^2] = \frac{\sigma_n^2 p_n}{N_0 ln2} = \sigma_n'^2$. The PDF of I can be obtained as $f_I(y) = f_{h'_1}(y) * f_{h'_2}(y) * \cdots * f_{h'_N}(y)$. The calculation of this multi-fold convolution is nontrivial. To avoid complicated computation, we

directly provide the following PDF and CDF of IMI as the calculation results as:

$$f_I(y) = \sum_{n=1}^{N} \frac{\sigma_n'^{2N-4}}{\prod_{i=1,i\neq n}^{N}(\sigma_n'^2 - \sigma_i'^2)} exp(-\frac{y}{\sigma_n'^2}) \tag{2.21}$$

$$F_I(y) = \sum_{n=1}^{N} \frac{-\sigma_n'^{2N-2}}{\prod_{i=1,i\neq n}^{N}(\sigma_n'^2 - \sigma_i'^2)} exp(-\frac{y}{\sigma_n'^2}) \tag{2.22}$$

These results can be easily obtained by using mathematical induction. From Equation (2.22), we can deduce the following theorem:

Theorem 2.1. *The optimal broadcast performance is achieved if and only if the power is allocated inversely proportional to the pass loss on each subcarrier. Under the power constraint* (2.4)*, it can be written as:*

$$p_i = \frac{\frac{1}{\sigma_i^2}}{\sum_{n=1}^{N}\frac{1}{\sigma_n^2}} P \quad i = 1, 2, \cdots, N \tag{2.23}$$

Proof. According to the analysis in Part II and Equation (2.3), we know that for the given outage probability q_0 and outage rate r_0, the coverage area is determined by IMIs CDF which is given by Equation (2.23). On the other hand, for a given value $y = y_0$, the optimal broadcast performance is reached if the corresponding power location scheme $(p_1, p_2, \cdots, p_N)$ minimizes $F_I(y_0)$.

Thus, in order to prove Theorem 1, it is equivalent to prove the Equation (2.22) is minimized for any $y = y_0$ if and only if the power allocated to each subcarrier is inversely proportional to σ_i^2. Mathematically, it can be written as:

$$p_i = \frac{\frac{1}{\sigma_i^2}}{\sum_{n=1}^{N}\frac{1}{\sigma_n^2}} P \quad i = 1, 2, \cdots, N$$

We prove above statement by mathematical induction. For $N = 2$, Equation (2.22) becomes:

$$F_I(p_1, p_2) = \frac{\sigma_1^2 p_1}{\sigma_2^2 p_2 - \sigma_1^2 p_1} e^{\frac{y_0 N_0 ln2}{-\sigma_1^2 p_1}} - \frac{\sigma_2^2 p_2}{\sigma_2^2 p_2 - \sigma_1^2 p_1} e^{\frac{y_0 N_0 ln2}{-\sigma_2^2 p_2}} \tag{2.24}$$

$$\mathbf{s.t.}: p_1 + p_2 = P \tag{2.25}$$

In order to find the optimal power allocation, we plug $p_1 = P - p_2$ into Equation (2.24). Take derivative of F_I with respect to p_2 and let $dF_I(p_2)/dp_2 = 0$, we have:

$$\begin{aligned} &\frac{\sigma_1^2\sigma_2^2 P + \frac{\sigma_1^2(P-p_2)}{p_2} y_0 N_0 ln2 - \sigma_2^2 y_0 N_0 ln2}{\sigma_1^2\sigma_2^2 P + \frac{\sigma_2^2(p_2)}{P-p_2} y_0 N_0 ln2 - \sigma_1^2 y_0 N_0 ln2} \\ &= exp[\frac{y_0 N_0 ln2}{\sigma_1^2(P-p_2)} - \frac{y_0 N_0 ln2}{\sigma_2^2 p_2}] \end{aligned} \tag{2.26}$$

The right part of the (2.26) is monotonically increasing with p_2 while the left part is monotonically decreasing. Thus we can verify that (2.26) is valid only when following condition holds:

$$\sigma_1^2(P - p_2) = \sigma_2^2 p_2 \tag{2.27}$$

which is the standard form of channel inversion for $N = 2$.

Using mathematical induction, suppose above result is valid for $N = k$, $\sigma_1^2 p_1 = \sigma_2^2 p_2 = \cdots = \sigma_k^2 p_k$. For $N = k + 1$, let p_{k+1} be the power allocated to the $k + 1$th subcarrier so that $P' = P - p_{k+1}$ is the total power allocated to the previous k subcarriers. For the previous k subcarriers, according the induction hypothesis, in order to optmizie the performance, the first k subcarriers should be allocated with power:

$$p_i = \frac{\frac{1}{\sigma_i^2}}{\sum_{n=1}^{k} \frac{1}{\sigma_n^2}}(P - p_{k+1}) \triangleq \frac{\frac{1}{\sigma_i^2}}{\sum_{n=1}^{k} \frac{1}{\sigma_n^2}} P' \tag{2.28}$$

Thus, we have $\sigma_i'^2 = \frac{p_i \sigma_i^2}{N_0 ln2} = \frac{1}{N_0 ln2 \sum_{n=1}^{k} \frac{1}{\sigma_n^2}} P'$ for any $1 \leq i \leq k$ and denote $\sigma_0^2 = 1/\sum_{n=1}^{k} \frac{1}{\sigma_n^2}$. Take (2.28) into Equation (2.22) and (2.35), we have:

$$\begin{aligned} F_I(P', p_{k+1}) = &(\frac{\sigma_0^2 P'}{\sigma_{k+1}^2 p_{k+1} - \sigma_0^2 P'})^k e^{\frac{y_0 N_0 ln2}{-\sigma_0^2 P'}} \\ &-(\frac{\sigma_{k+1}^2 p_{k+1}}{\sigma_{k+1}^2 p_{k+1} - \sigma_0^2 P'})^k e^{\frac{y_0 N_0 ln2}{-\sigma_{k+1}^2 p_{k+1}}} \end{aligned} \tag{2.29}$$

$$\mathbf{s.t.}: P' + p_{k+1} = P \tag{2.30}$$

In order to find the optimal power allocation, we take $P' = P - p_{k+1}$ into Equation (2.29). Take derivative of F_I with respect to p_{k+1} and let $dF_I(p_{k+1})/dp_{k+1} = 0$, we have:

$$\begin{aligned} &\frac{k\sigma_0^2\sigma_{k+1}^2 P + \frac{\sigma_{k+1}^2 p_{k+1}}{P-p_{k+1}} y_0 N_0 ln2 - \sigma_{k+1}^2 y_0 N_0 ln2}{k\sigma_0^2\sigma_{k+1}^2 P + \frac{\sigma_2^2 (P-p_{k+1})}{p_{k+1}} y_0 N_0 ln2 - \sigma_0^2 y_0 N_0 ln2} \\ &= [\frac{\sigma_0^2(P-p_{k+1})}{\sigma_{k+1}^2 p_{k+1}}]^{k-1} exp[\frac{y_0 N_0 ln2}{\sigma_{k+1}^2 p_{k+1}} - \frac{y_0 N_0 ln2}{\sigma_0^2(P-p_{k+1})}] \end{aligned} \tag{2.31}$$

The right part of (2.31) is monotonically decreasing with p_{k+1} while the left part is monotonically increasing. Thus we can verify that (2.31) is valid only when the following condition holds:

$$\sigma_0^2(P - p_{k+1}) = \sigma_{k+1}^2 p_{k+1} \tag{2.32}$$

Notice that $\sigma_0^2 = 1/\sum_{n=1}^{k} \frac{1}{\sigma_n^2}$ and take (2.32) into (2.30), we have:

$$p_{k+1} = \frac{\frac{1}{\sigma_{k+1}^2}}{\frac{1}{\sigma_{k+1}^2} + \sum_{n=1}^{k} \frac{1}{\sigma_n^2}} P = \frac{\frac{1}{\sigma_{k+1}^2}}{\sum_{n=1}^{k+1} \frac{1}{\sigma_n^2}} P \tag{2.33}$$

$$p_i = \frac{\frac{1}{\sigma_i^2}}{\sum_{n=1}^{k} \frac{1}{\sigma_n^2}} (P - p_{k+1}) = \frac{\frac{1}{\sigma_i^2}}{\sum_{n=1}^{k+1} \frac{1}{\sigma_n^2}} P \quad i = 1, 2, \cdots, k \tag{2.34}$$

This is exactly the form of channel inversion power allocation scheme for $N = k + 1$. Therefore, Theorem 1 is proved. □

Theorem 1 shows that in the low SNR regime, the optimal performance is reached when the power allocated among subcarriers reaches a "balance" ($\sigma_1^2 P_1 = \sigma_2^2 P_2 = \cdots = \sigma_N^2 P_N$).

Note that in Equation (2.23), $\sigma_i'^2 \neq \sigma_j'^2$ for any $i \neq j$. In the optimal case where $\sigma_1'^2 = \sigma_2'^2 = \cdots = \sigma_N'^2 = \sigma'^2$, Equation (2.21) becomes:

$$f_I(y) = \frac{y^{N-1}}{(N-1)!\sigma'^{2N}} exp(-\frac{y}{\sigma'^2}) \tag{2.35}$$

When the number of subcarriers N is large, (2.21)-(2.22) are still complicate to calculate. In order to compute the PDF of IMI for large N, we use the *Central Limit Theorem* to approximate $I(\overrightarrow{h}, \overrightarrow{p})$ as a Gaussian random variable. We only need to calculate the mean and variance of $I(\overrightarrow{h}, \overrightarrow{p})$, which are given as:

$$E[I] = \frac{1}{N_0 ln2} \sum_{n=1}^{N} p_n \sigma_n^2 \tag{2.36}$$

$$E[I^2] = \frac{1}{(N_0 ln2)^2} [\sum_{n=1}^{N} p_n^2 \sigma_n^4 + \sum_{n \neq m} p_n p_m \sigma_n^2 \sigma_m^2] \tag{2.37}$$

then we can use the Gaussian distribution to approximate the PDF of IMI.

2.2.3. IMI in high SNR condition

If SNR is large, IMI can be written as:

$$I(\overrightarrow{h}, \overrightarrow{p}) = \sum_{n=1}^{N} [\frac{B_n}{ln2} ln(SNR_n)] \tag{2.38}$$

Rewrite Equation (2.38), we get the following form:

$$I(\overrightarrow{h}, \overrightarrow{p}) = \sum_{n=1}^{N} B_n [log_2(p_n)] + \sum_{n=1}^{N} B_n [log_2(\frac{|h_n|^2}{N_0 B_n})] \tag{2.39}$$

In Equation (2.39), once power allocation is completed, the term $\sum_{n=1}^{N} [log_2(p_n)]$ is a constant and rest part $\sum_{n=1}^{N} [log_2(\frac{|h_n|^2}{N_0 B_n})]$ is a random variable solely determined by $|h_n|^2$. The value of $\sum_{n=1}^{N} [log_2(p_n)]$ will only affect the position of the PDF curve

without changing its shape. Thus, in order to maximize the broadcast coverage, we should maximize $\sum_{n=1}^{N}[log_2(p_n)]$. According to arithmetic inequality:

$$\sum_{n=1}^{N}[log_2(p_n)] = log_2[\prod_{n=1}^{N} p_n] \leq Nlog_2(\frac{P}{N}) \tag{2.40}$$

The equality can be reached if and only if the power is equally allocated among subcarriers:

$$p_i = \frac{P}{N} \quad i = 1, 2, \cdots, N \tag{2.41}$$

So we have shown that simple equal power allocation among subcarriers can optimize the broadcast performance in high SNR regime. Since SNR_n is deterministic at the transmitter, we only need to focus on $\sum_{n=1}^{N} ln(|h_n|^2)$ to determine the distribution of I . Based on (2.11), the PDF of $y = ln(|h_n|^2)$ is:

$$f_n(y) = \frac{1}{\sigma_n^2} exp(y - \frac{e^y}{\sigma_n^2}) \tag{2.42}$$

Similar to steps (2.11)-(2.18), we can get the lower bound of the PDF of IMI as:

$$exp(y - \frac{e^y}{\sigma_N^2}) \prod_{n=1}^{N-1} [\Gamma(0, \frac{1}{\sigma_n^2}) - \Gamma(0, \frac{1}{\sigma_{n+1}^2})] \tag{2.43}$$

and the upper bound is:

$$exp(y - \frac{e^y}{\sigma_1^2})[\Gamma(0, \frac{1}{\sigma_N^2}) - \Gamma(0, \frac{e^y}{\sigma_N^2})] \prod_{n=2}^{N-1} [\Gamma(0, \frac{1}{\sigma_n^2}) - \Gamma(0, \frac{1}{\sigma_{n+1}^2})] \tag{2.44}$$

where $\Gamma(0, x)$ is defined in Equation (2.19).

2.3. Broadcast system with Multiple Antennas

In a broadcast network, the broadcast station (BS) or receiver may be equipped with multiple antennas. Meanwhile, multiple BS can form a distributed virtual multi-

antenna system to collaboratively transmit the broadcast signal. For a broadcast network with multiple antennas (distributed or centralized), the IMI in Equation (2.3) becomes:

$$I(\mathbf{H}, \mathbf{Q}) = Blog_2 det(\mathbf{I} + \frac{\mathbf{HQH^H}}{N_0 B}) \tag{2.45}$$

where $\mathbf{H}$ is the channel gain matrix associated with user w (on the boundary of the coverage area A); $\mathbf{I}$ is the identity matrix and $\mathbf{Q} = E[\overrightarrow{x}\overrightarrow{x}^H]$ is the covariance matrix of the input signals.

The IMI analysis in the general MIMO channel is difficult so we focus on the following practical cases.

2.3.1. IMI in Multiple BS

In this subsection, we assume a broadcast network with N_t BS where each BS is subject to an individual power constraint (2.4). By symmetry, each BS has the same power allocation strategy over subcarriers. With multiple BS, we consider two transmission schemes: SFN and multiple BS collaboration (MBC).

In SFN, multiple BS send the same signal over the same frequency channel at the same time. In this case, the effective channel gain on subcarrier n for user w becomes $\sum_{m=1}^{N_t} \sqrt{p_n} h_n(m)$. Accordingly, q^w in SFN is expressed as:

$$q^w = Prob[\overrightarrow{h_n} : \sum_{n=1}^{N} B_n log_2(1 + \frac{p_n |\sum_{m=1}^{N_t} h_n(m)|^2}{N_0 B_n}) \leq r_0] \tag{2.46}$$

In (2.47), since $|h_n(1)|, |h_n(2)|, \cdots, |h_n(N_t)|$ are independent complex Gaussian random variables, the new equivalent channel gain $\sqrt{\sum_{m=1}^{N_t} h_n(m)}$ also follows Raleigh distribution. Therefore, all the results in Section III are applicable to SFN where $\sigma_n = \sum_{m=1}^{N_t} \sigma_n^2(m)$.

In MBC, multiple BS fully collaborate to form a distributed multiple input single output (MISO) system. Accordingly, the outage probability q^w is [29]:

$$q^w = Prob[\overrightarrow{h} : \sum_{n=1}^{N} B_n log_2 det(\mathbf{I} + \frac{\overrightarrow{h_n}\mathbf{Q_n}\overrightarrow{h_n}^H}{N_0 B_n}) \leq r_0] \tag{2.47}$$

$$\mathbf{s.t.}: \quad Trace(\mathbf{Q_n}) = p_n$$
$$\textstyle\sum_{n=1}^{N} p_n = P$$

where $\overrightarrow{h_n} = [h_n(1), h_n(2), \cdots, h_n(N_t)]$ is the channel gain on nth subcarrier from BS to receiver w; $\mathbf{Q_n} = E[\overrightarrow{x_n}^H \overrightarrow{x_n}]$ is the input covariance matrix. In the case of low SNR, the IMI in (2.47) can be written as:

$$I(\overrightarrow{h}, \overrightarrow{p}) = \frac{1}{N_0 ln2} \sum_{k=1}^{N} \sum_{n=1}^{N_t} p_k(n)|h_k(n)|^2 = \frac{1}{N_0 ln2} \sum_{n=1}^{N_t} \sum_{k=1}^{N} p_k(n)|h_k(n)|^2 \tag{2.48}$$

From Equation (2.48), we can see that each BS independently contributes to the IMI. In other words, for any receiver in the coverage area, the overall IMI can be optimized by maximizing the individual term $\sum_{k=1}^{N} p_k(n)|h_k(n)|^2$ of each BS.

Using similar approach as of (2.20) to (2.22), we can derive the PDF of IMI in Equation (2.48) as:

$$f_{I,MBC}(y) = \sum_{k=1}^{N} \sum_{n=1}^{N_t} \frac{\sigma_k''(n)^{2N-4}}{\prod_{i=1}^{N} \prod_{j=1,(i,j)\neq(k,n)}^{N_t} [\sigma_k''(n)^2 - \sigma_i''(j)^2]} exp[\frac{-y}{\sigma_k''(n)^2}] \tag{2.49}$$

where $\sigma_k''(n)^2 = \frac{\sigma_k(n)^2 p_k(n)}{ln2 N_0 N_t}$ and $|h_k''(n)|^2 = \frac{p_k(n)}{ln2 N_0 N_t}|h_k(n)|^2$. From Theorem 1, we have the following corollary on the optimal power allocation scheme in MBC:

Corollary 2.1. *In low SNR regime, the optimal MBC broadcast performance is achieved if and only if the power is allocated inversely proportional to the pass loss on*

each subcarrier over all base stations, it can be written as:

$$p_k(n) = \frac{\frac{1}{\sigma_k(n)^2}}{\sum_{i=1}^{N}\sum_{j=1}^{N_t}\frac{1}{\sigma_i(j)^2}}P, \quad k = 1, 2, \cdots, N \quad n = 1, 2, \cdots, N_t \tag{2.50}$$

2.3.2. IMI with Multiple Receiving Antennas

For convenience of our discussion, we assume all the users in a SIMO system have the same number of receiving antenna N_r, thus we change matrix $\mathbf{H}$ in Equation (2.45) with vector $\overrightarrow{h}' = [h(1), h(2), \cdots, h(N_r)]^H$ where w still represents the worst user on the edge of the coverage area. Accordingly, Equation (2.45) becomes:

$$I(\overrightarrow{h}) = Blog_2 det(\mathbf{I} + \frac{\overrightarrow{h}' P \overrightarrow{h}}{N_0 B}) = Blog_2[1 + \frac{P}{N_0 B}\sum_{i=1}^{N_r}|h(i)|^2] \tag{2.51}$$

Since $h(i)$ is the channel gain from the ith BS to the receiver w, it also can be seen as the Rayleigh distribution, so $|h(i)|^2$ is chi-square distributed. According to the result of Equation (2.21), we can get the distribution of $z = \sum_{i=1}^{N_r}|h(i)|^2$:

$$f(z) = \sum_{n=1}^{N_r}\frac{\sigma(n)^{2N_r-4}}{\prod_{i=1,i\neq n}^{N_r}[\sigma(n)^2 - \sigma(i)^2]}exp[\frac{-z}{\sigma(n)^2}] \tag{2.52}$$

Now, for $Z_k = B_k log_2[1 + \frac{p_k}{N_0 B_k}\sum_{i=1}^{N_r}|h_k(i)|^2]$, we have:

$$F(Z_k \leq z_0) = F[\sum_{i=1}^{N_r}|h_k(i)|^2 \leq (2^{z_0/B_k} - 1)\frac{N_0 B_k}{p_k}] \tag{2.53}$$

Taking derivative on both sides so we can get the PDF of Z_k and the distribution of IMI:

$$\begin{aligned} f_{Z_k}(z_0) &= \frac{N_0 ln2}{p_k}2^{z_0/B_k} f[(2^{z_0/Bk} - 1)\frac{N_0 B_k}{p_k}] \\ &= \frac{N_0 ln2}{p_k}2^{z_0/B_k}\sum_{n=1}^{N_r}\frac{\sigma_k(n)^{2N_r-4}}{\prod_{i=1,i\neq n}^{N_r}[\sigma_k(n)^2 - \sigma_k(i)^2]}exp[\frac{(1-2^{z_0/B_k})\frac{N_0 B_k}{p_k}}{\sigma_k(n)^2}] \end{aligned} \tag{2.54}$$

$$f_I(t) = \frac{N_0 ln2}{P} 2^{\frac{t}{B}} \sum_{n=1}^{N_r} \frac{\sigma(n)^{2N_r-4}}{\prod_{i=1,i\neq n}^{N_r}[\sigma(n)^2 - \sigma(i)^2]} exp[\frac{(2^{\frac{t}{B}}-1)\frac{N_0 B}{P}}{\sigma(n)^2}] \tag{2.55}$$

Using Equation (2.55), we can determine the coverage area for given q^0 and r^0. For multicarrier, the IMI has the following form:

$$I(\overrightarrow{h}, \overrightarrow{p}) = \sum_{n=1}^{N} B_n log_2[1 + \frac{p_n}{N_0 B_n} \sum_{i=1}^{N_r} |h_n(i)|^2] = \sum_{k=1}^{N} Z_k \tag{2.56}$$

Thus in multicarrier scenario, the PDF of IMI is determined as follow:

$$f_I(t) = f_{Z_1}(t) * f_{Z_2}(t) * \cdots f_{Z_N}(t) \tag{2.57}$$

where "*" statnds for convolution and $f_{Z_k}(t)$ has the form as in Equation (2.54). Since in low SNR condition, $Z_k = \frac{P_k}{N_0 ln2} \sum_{i=1}^{N_r} |h_k(i)|^2$, IMI can be written as:

$$I(\overrightarrow{h}, \overrightarrow{p}) = \sum_{k=1}^{N} Z_k = \frac{1}{N_0 ln2} \sum_{k=1}^{N} \sum_{i=1}^{N_r} p_k |h_k(i)|^2 \tag{2.58}$$

Similar as Equation (2.20) and (2.21), we can derive the pdf of IMI in low SNR condition as:

$$f_I(t) = \sum_{k=1}^{N} \sum_{n=1}^{N_r} \frac{\sigma'_k(n)^{2NN_r-4}}{\prod_{j=1}^{N} \prod_{i=1,(j,i)\neq(k,n)}^{N_r}[\sigma'_k(n)^2 - \sigma'_j(i)^2]} exp[-\frac{t}{\sigma'_k(n)^2}] \tag{2.59}$$

where $\sigma'_k(n)$ has same definition as in Equation (2.21). In a practical SIMO system, due to the size limitaion of the receiver, the antennas on receiver has very small spacing. Thus, it is reasonable for us to assume $|h_k(1)|, |h_k(2)|^2 \cdots |h_k(N_r)|^2$ are $i.i.d$

and chi-square distributed on each subcarrier. Thus, Equation (2.58) becomes:

$$I(\overrightarrow{h}, \overrightarrow{p}) = \frac{1}{N_0 ln2} \sum_{k=1}^{N} p_k \sum_{i=1}^{N_r} |h_k(i)|^2 \tag{2.60}$$

where $\sum_{i=1}^{N_r} |h_k(i)|^2$ follows chi-square distribution. Thus, equation (2.60) has similar form as (2.20) and Theorem 1 also applies to (2.60) for optimal power allocation in SIMO system.

2.4. Simulations and discussion of results

In this section, numerical results are provided to evaluate the performance of the broadcast system under different network configurations. We use the Hata model [31] for calculating the large scale path loss. The empirical path loss in urban areas can be expressed as:

$$\begin{aligned} P_L(d)dB = 69.55 + 26.16log_{10}(f_c) - 13.82log_{10}(h_t) \\ - a(h_r) + [44.9 - 6.55log_{10}(h_t)]log_{10}(d) \end{aligned} \tag{2.61}$$

where f_c is the carrier frequency, h_t and h_r are the height of the transmitter and receiver antenna, respectively, and d is the distance between the transmitter and receiver. In big cities at frequencies $f_c > 300$ MHz, the correction factor $a(h_r)$ is given by:

$$a(h_r) = 3.2[log_{10}(11.75h_r)]^2 - 4.97 \tag{2.62}$$

From (2.61), the average received power at distance d is:

$$2\sigma^2 = P10^{P_L(d)/10} \tag{2.63}$$

where P is the transmitted power.

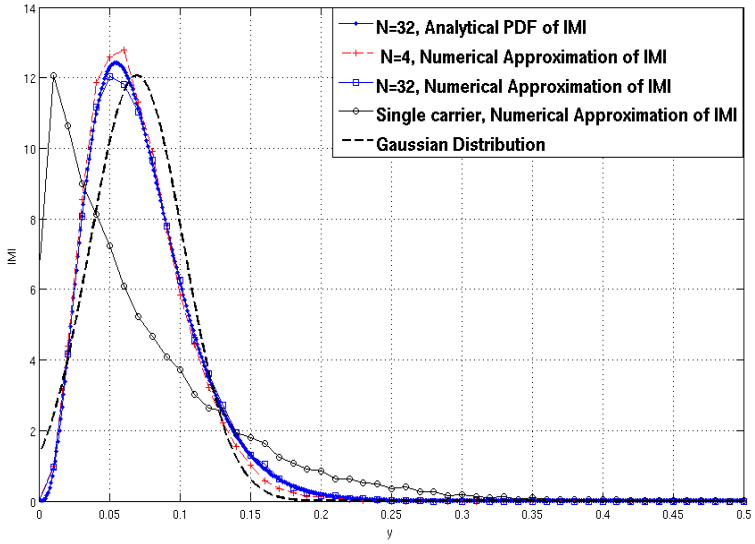

Figure 2.2. Probability distributions of IMI

Without loss of generality, we can choose the broadcast $r^0 = 515$ Kbps and the total power to be $P = 1$ watt such that the radius $d = 1$ km is the benchmark distance with outage probability $q_0(d_0) = 5\%$. Figure 2.2 shows the distribution of IMI in the low SNR region with $N = 4$. Compared to the single carrier case, the performance of multicarrier with joint coding is much better. Also, we can see the PDF of IMI is close to the Gaussian approximation, which is expected according to the Central Limit Theorem. The simulation results match our analysis equation (2.38) and (2.39) very well.

In a single cell broadcast network, Figure 2.3 shows the relationship between the number of subcarriers (N) and the coverage area with different SNR and outage probabilities (q_0). Apparently, the coverage area increases with q_0. As expected, the added frequency diversity in multicarrier transmission with joint coding provides significant coverage increment compared with the single carrier case. However, we observe that the coverage incremental rate decreases with N due to the diminishing return on frequency diversity. Also, in the low SNR regime, the coverage area is less

sensitive to N and q_0 because the additive Gaussian noise in the channel becomes the dominant factor affecting the broadcast performance.

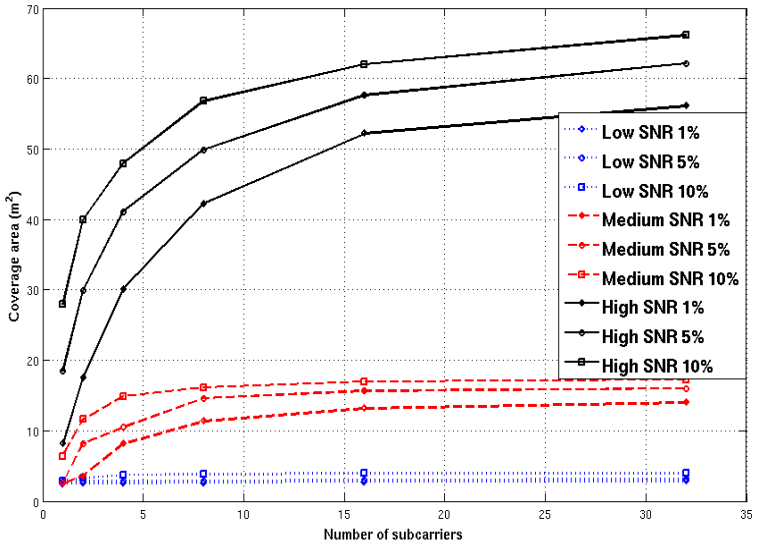

Figure 2.3. Broadcast coverage areas of single cell

For multi-cell broadcast networks, Figure 2.4 and 2.5 show the actual broadcast coverage with two and three base stations respectively. In both cases, we assume the base stations are placed symmetrically with distance of 1 km from the origin. We can see the coverage area of MBC multicarrier (MBC-MC) is the largest in both cases. This is due to the full exploitation of the transmission diversity in both frequency and space. We also present the broadcast coverage for single BS located in the origin. It is easy to see that by adopting multiple antenna at the receiver or using multi-carrier transmission, we can achieve significant performance improvement. Additionally, Figure 2.6 and 2.7 show the coverage areas of the MBC and SFN with different N and q_0 in the medium SNR regime. Similar to Figure 2.3, the coverage curves in Figure 2.7 and 2.8 have steep slops with small N but become flat when $N > 16$. Also, in Table 2.1, we have given the numerical values for the coverage of three cells under different transmission strategy and we can see that MBC-MC has the largest coverage area.

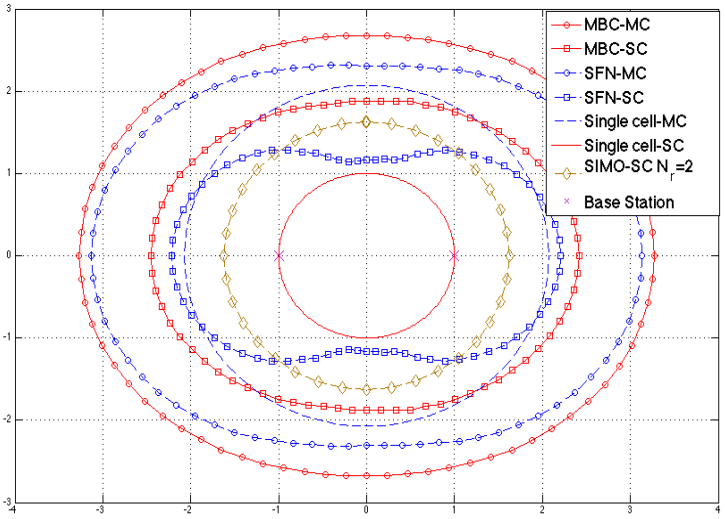

Figure 2.4. Broadcast coverage of two cells (N=8, $q^0 = 5\%$)

Table 2.1. Broadcast coverage area of three cells

Outage	MBC-MC	MBC-SC	SFN-MC	SFN-SC	SC-MC
$q^0 = 0.01$	39.143	23.795	31.241	13.764	13.461
$q^0 = 0.05$	35.503	16.403	26.971	7.215	10.869

In multi-cell broadcast networks, the BS separation distance (denoted as D) also plays a key role in determining the coverage area. Figure 2.8 and 2.9 show the total coverage area as a function of D under different transmission schemes. We notice that when D increases, the coverage area first increases but then decreases after reaching its maximum. Intuitively, this makes sense because achieving the spatial diversity gain requires certain distance among BSs. However, collaboration among the BSs becomes weak with increased D. When D is large enough, multiple BSs cannot collaborate with each other and the total coverage area becomes the sum of the coverage area of each individual cell. From Figure 2.8 and 2.9, we can see the optimal separation distance is about twice the radius of the single cell coverage.

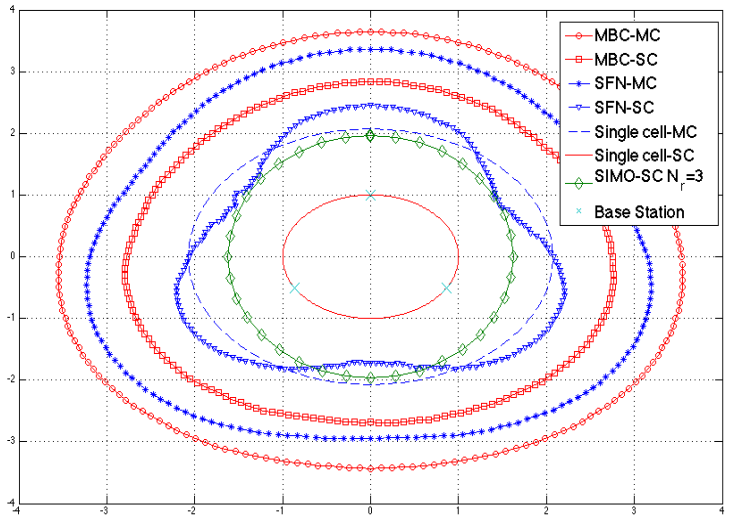

Figure 2.5. Broadcast coverage of three cells (N=8, $q^0 = 5\%$)

Figure 2.10 to Figure 2.13 show the broadcast performance under three different power allocation schemes: (i) equal power allocation among subcarriers; (ii) inverse allocation according to Equation (2.24); (iii) proportional allocation where the power assigned to subcarrier i is proportional to σ_i^2. For comparison purpose, in each figure we normalize the coverage area of equal power allocation with $q^0 = 1\%$ to 1. We can see that the simulation results match our analysis in previous very good. Specifically, in low SNR regime, the inverse power allocation provides the largest coverage area. In high SNR regime, the equal power allocation becomes the optimum. In multi-cell broadcast network, Figure 2.12 and 2.13 confirm the MBC transmissions always outperform the SFN transmissions at arbitrary SNR.

2.5. Summary

In this chapter, we studied the performance of multicarrier broadcast systems with joint coding over subcarriers. The outage capacity and the coverage area were chosen to be the figure of merit. A thorough analysis of the IMI that solely determines the maximum broadcast coverage area is provided for power allocation.

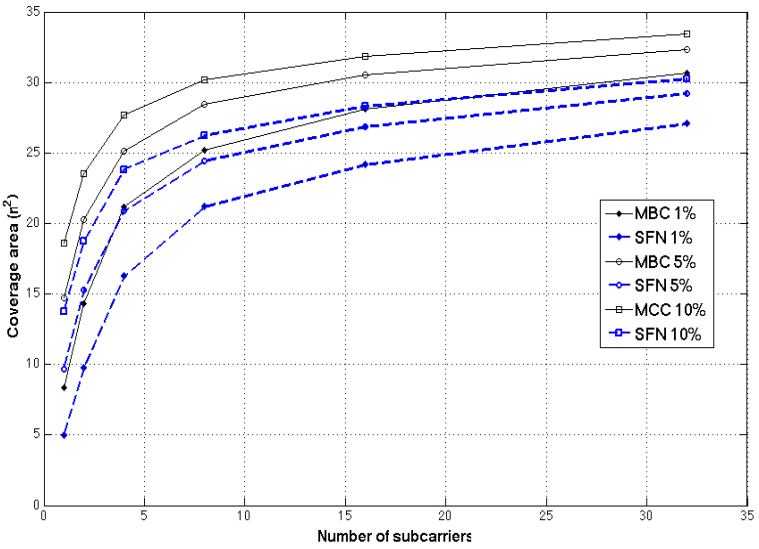

Figure 2.6. Broadcast coverage areas of two-cell with different schemes

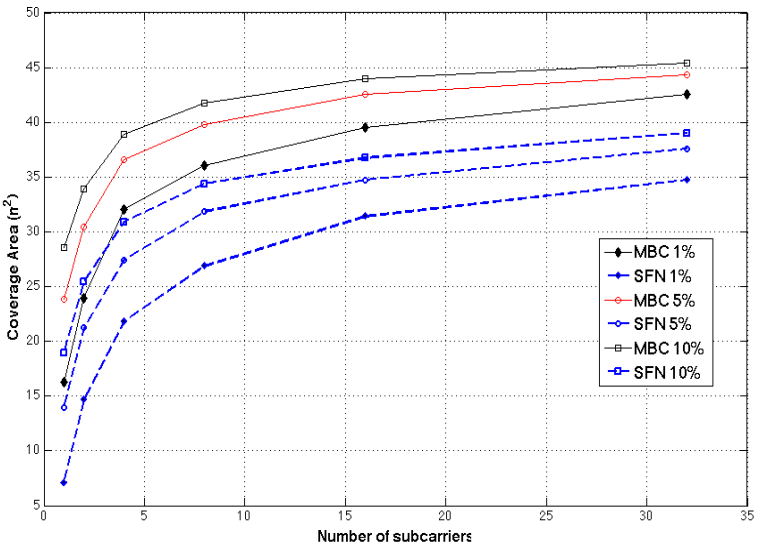

Figure 2.7. Broadcast coverage areas of three-cell with different schemes

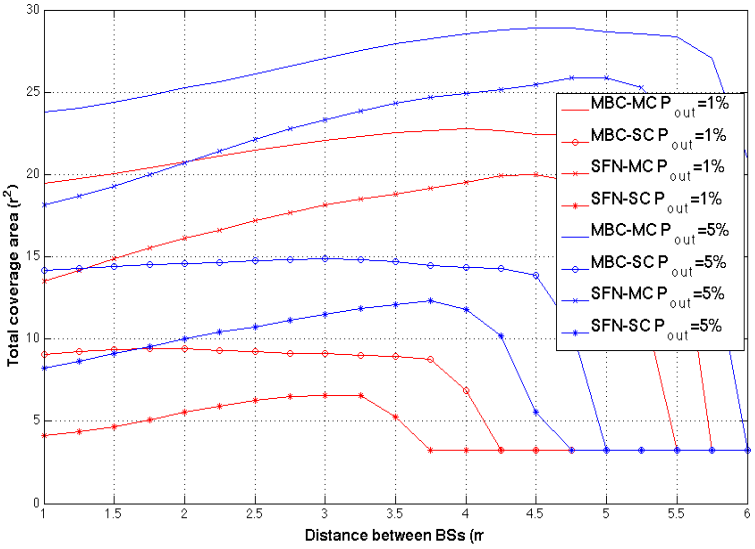

Figure 2.8. Coverage areas of two cells under different BS separation distance

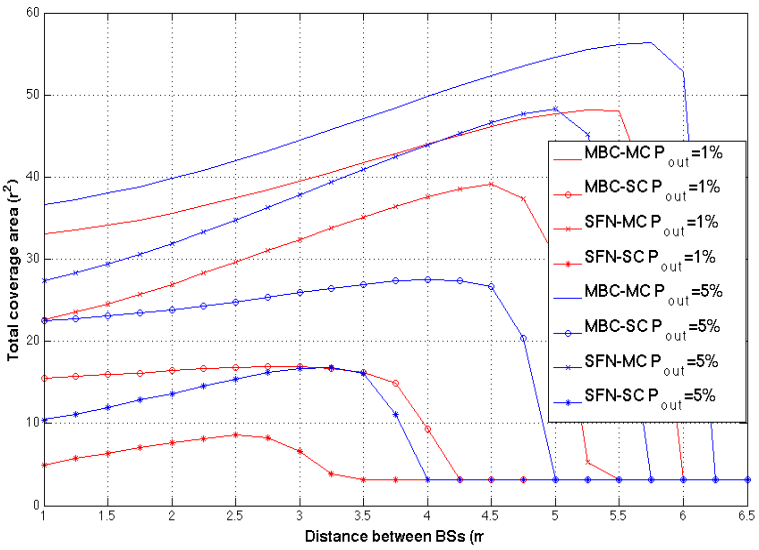

Figure 2.9. Coverage areas of three cells under different BS separation distance

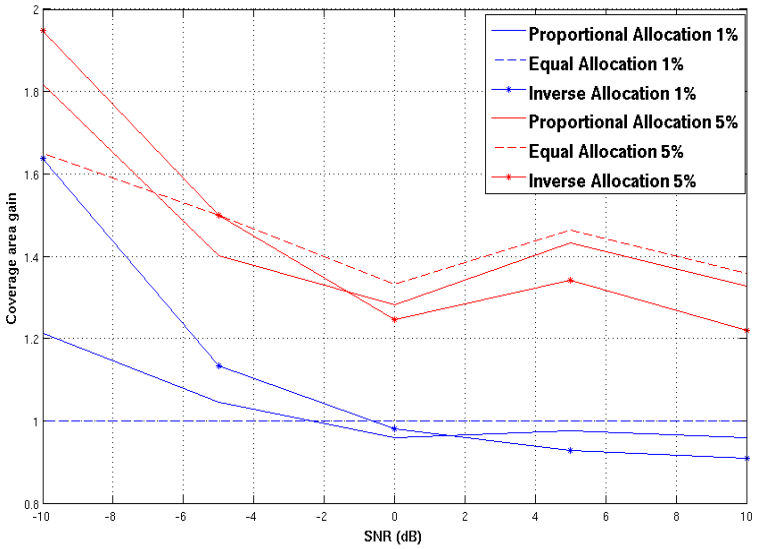

Figure 2.10. Coverage areas gains of single cell, $N = 4$

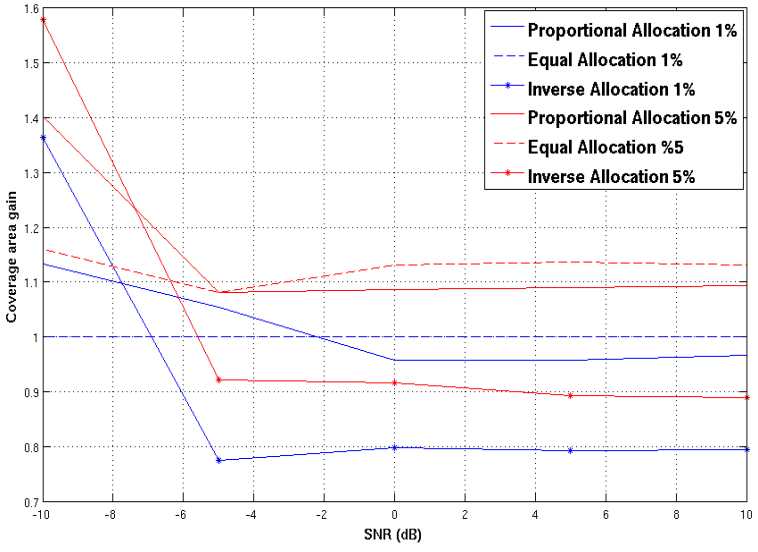

Figure 2.11. Coverage areas gains of single cell, $N = 16$

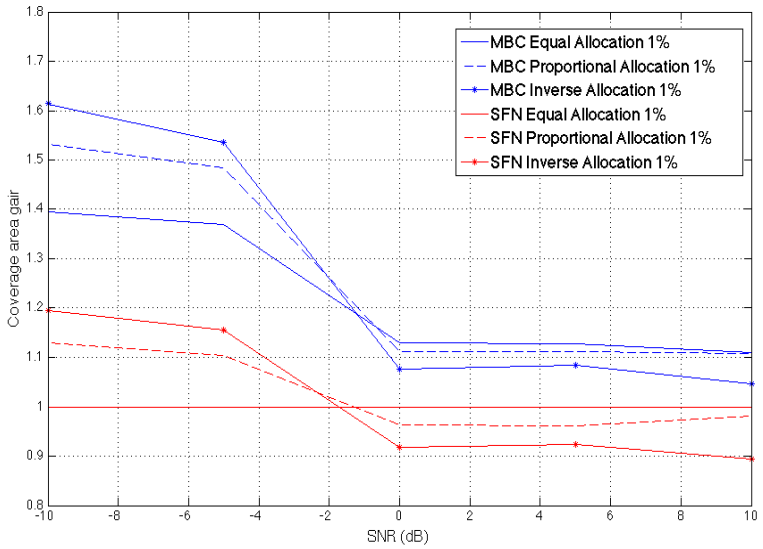

Figure 2.12. Coverage areas gains of two cells ($N = 4$ and $q^0 = 1\%$)

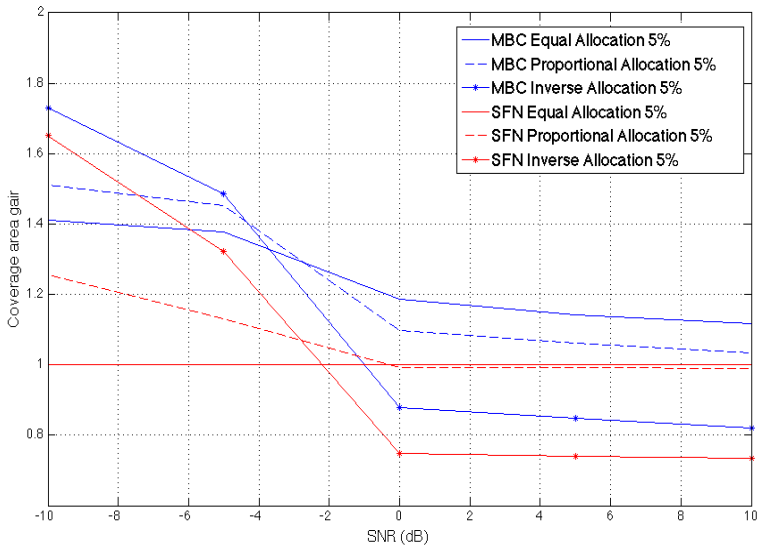

Figure 2.13. Coverage areas gains of two cells ($N = 4$ and $q^0 = 5\%$)

CHAPTER 3. OPTIMAL DPC SCHEME IN HYBRID NETWORK

Recent years, wireless communication is experiencing an explosive increase in the number of mobile devices and real time multimedia applications. With the prevalence of the smart phones and tablets, major wireless providers (e.g., Verizon, Sprint, and T-mobile) are offering both mobile TV (broadcast) and 3G/4G broadband internet access (unicast) services. Also, the TV services can be further categorized according to different quality or resolutions (e.g. HDTV 1080p, HDTV 720p and SDTV). In some countries such as China, Japan and Germany, researches on offering HDTV and SDTV through cellular network are already in progress [54] [55]. As a result, hybrid cellular has become an intriguing concept where it integrates the broadcast and unicast services into a single infrastructure [56]. Compared to broadcast, unicast has the advantage of consuming resources only when a user is actively using the network service. Also, with unicast, the network can optimize the transmission based on the CSI for individual users. However, the unfavorable scaling behavior of unicast [57] can become a serious issue when many users are watching TV at the same time. Apparently, broadcast technology is more resource efficient for high demand mobile TV services since a single broadcast transmission will accommodate all users simultaneously [58]. Due to their inherent differences, the broadcast and unicast networks have evolved along different trajectories [59].

The hybrid network aims to provide a single platform to collaboratively deliver both broadcast and unicast services. We assume the broadcast and unicast signals are of equal importance and they share the same transmitter: the base station (BS), which makes time and spectrum sharing a reality. However, existing orthogonal resource sharing schemes (TDMA, OFDMA) have low spectrum utilization efficiency [60]. In order to enhance the spectrum efficiency, a broadcast and unicast overlaid system using superposition coding was introduced in [61]. However, the use of superposition

coding requires successive interference cancellation at each receiver, which is not practical for power limited mobile terminals. Recently, Dirty Paper Coding (DPC) has gained significant attention because it can achieve multiuser downlink capacity with simple receiver structure [62] - [65]. Since the broadcast and unicast signals in hybrid cellular are transmitted by the same BS, one signal can be modeled as known interference to the other so that the transmission system can be perfectly cast into the DPC framework. In [66] , [67], we introduced a DPC-based collaborative transmission scheme for a general multicarrier broadcast and unicast hybrid system and show that it has significant capacity gains over orthogonal access schemes.

In a multiuser unicast only system where the channels are degraded, the optimal DPC interference pre-cancellation always protects the users with better channel quality. In the DPC based hybrid system described in[66] and [67], only outage capacity is considered for broadcast network such that the optimal interference pre-cancellation order can also be determined by comparing unicast channel gain with broadcast channel threshold. To the best of our knowledge, the optimal DPC interference pre-cancellation order for broadcast and unicast hybrid network with ergodic capacity region has not yet been studied. In this part, we analytically derive the optimal DPC interference pre-cancellation order in broadcast and unicast hybrid cellular network. Unlike unicast only system, our results show that the optimal DPC interference pre-cancellation order is not always fixed, but depends on a number of factors including channel gains and the signal to noise ratio of each signal.

3.1. Hybrid network model

In order to measure the hybrid network performance, from an information theoretic point of view, we use channel capacity as the figure of merit. In particular, we consider a broadcast and unicast (downlink only) hybrid network where the base station delivers M broadcast signal and K unicast signals. In information theory,

there are two channel capacity definitions that are relevant to the system design for a broadcast channel with an uninformed transmitter: for fast fading channels, the ergodic capacity defines the maximum data rate that can be sent to the receiver with asymptotically small error probability through all fading states; for slow fading channels, the outage capacity defines the maximum data rate that can be transmitted with certain outage probability that the received data can not be decoded with negligible error probability. If the received signal to noise ratio (SNR) is above the threshold corresponding to the outage probability, the transmitted data can be decoded with negligible probability of error; otherwise, the transmission is in outage. In this chapter, we consider both ergodic capacity and outage capacity for broadcast. In contract to broadcast, unicast can optimize its transmission based on instantaneous CSI at the transmitter so that we use the Shannon capacity as the unicast performance metric.

We assume there are M number of broadcast signals and denote the common information broadcast rates as $R^b(1), R^b(2), \cdots, R^b(M)$ and the number of broadcast receivers can be arbitrary. We assume there are totally K unicast signals and the private information rate for unicast user k is defined as $R^u(k)$. Then the hybrid capacity region is:

$$C_{hybrid} = [R^b(1), R^b(2), \cdots, R^b(M), R^u(1), R^u(2), \cdots, R^u(K)] \tag{3.1}$$

$$\mathbf{s.t.}: \sum_{n=1}^{M} P^b(i) + \sum_{n=1}^{K} P^u(k) \leq P \tag{3.2}$$

where $P^b = \sum_{n=1}^{M} P^b(i)$ and $P^u = \sum_{n=1}^{K} P^u(k)$ are the transmit power for broadcast and unicast respectively. $P^b(i)$ is the transmit power assigned to the ith broadcast signal and $P^u(k)$ is the transmit power assigned to the kth unicast user. Note that in our hybrid network, the same transmitter sends both BC and UC signals, so

the hybrid capacity region is subject to the total power constraint in (2), which is imposed by the radio frequency (RF) amplifier under the assumption of zero power loss at the transmitter. For the convenience of discussion, we assume single frequency transmission, i.e., M broadcast signal and K unicast signals share the same channel via DPC interference pre-cancellation.

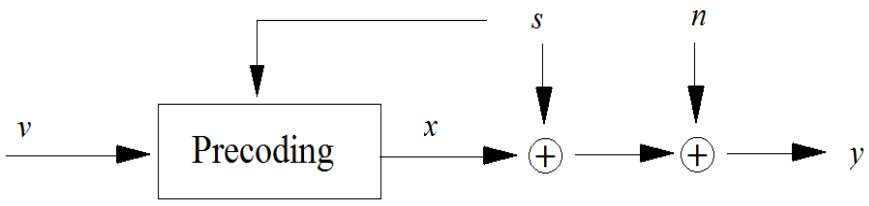

Figure 3.1. Dirty paper pre-codings

The basic principle of DPC is illustrated in Figure 3.1. Assume v is the desired signal to be transmitted, s is the interference and n is the AWGN noise. If the interference s is non-causally known at the transmitter, the Costa's results show that by adding a pre-coder at the transmitter, the receiver can demodulate source v as if the interference were not present. That is, the capacity of the interference channel is the same as that of the AWGN channel without interference. In the hybrid cellular, since the broadcast and unicast share the same transmitter (BS), one signal can be viewed as known "interference" to the other signal. Therefore, the hybrid transmission can be perfectly cast into the DPC framework, resulting in an overlaid hybrid network architecture [66]. The notion of transmitter-based interference pre-cancellation turned to be the key to share the same channel between broadcast and unicast.

3.2. Hybrid network with single carrier transmission

In the hybrid network, since the unicast channel gains are degraded and known by the transmitter, the interference pre-cancellation order among unicast users can

be easily determined. That is, for arbitrary two unicast user i and j, the capacity optimal DPC operation is to treat user j's signal as interference and pre-cancel this interference from user i if $|h^u(i)|^2 > |h^u(j)|^2$ [68]. Since the transmitter only knows the broadcast channel statistics, the challenge is to determine the interference pre-cancellation order between broadcast and unicast signals. For the convenience of discussion, we first study the simplest one broadcast and one unicast (1BC+1UC) hybrid scenario, which will provide useful insights for the general case.

3.2.1. Hybrid network with single BC

When the network only consists of one broadcast signal and one unicast signal, we can drop the signal indices and simply denote the broadcast signal as b and the unicast signal as u. Then the hybrid capacity region (3.1)-(3.2) become:

$$C_{hybrid} = [R^b, R^u] \tag{3.3}$$

$$\mathbf{s.t.}: P^b + P^u = P \tag{3.4}$$

Under DPC operation, only two interference cancellation orders are possible: (1) BC is pre-canceled from UC; (2) UC is pre-canceled from BC. We denote the achievable rate regions obtained from these two schemes as C^1_{hybrid} and C^2_{hybrid} respectively.

For broadcast ergodic capacity, according to Shannon's formula, the achievable rate region C^1_{hybrid} and C^2_{hybrid} can be written as:

$$C^1_{hybrid} = [R^b_1, R^u_1] = \{E[Blog_2(1 + \frac{P^b_1|h^b|^2}{N_0B + P^u_1|h^b|^2})], Blog_2(1 + \frac{P^u_1|h^u|^2}{N_0B})\} \tag{3.5}$$

$$C^2_{hybrid} = [R^b_2, R^u_2] = \{E[Blog_2(1 + \frac{P^b_2|h^b|^2}{N_0B})], Blog_2(1 + \frac{P^u_2|h^u|^2}{N_0B + P^b_2|h^u|^2})\} \tag{3.6}$$

where B is the bandwidth and N_0 is the Gaussian white noise spectrum density. The first terms of (3.5) and (3.6) are the broadcast ergodic rates, where E stands for

expectation because h^b is a random variable. Note that for given P^b and P^u, the transmitter fixes the broadcast ergodic rate but varies the unicast rate according to the instantaneous h^u. Our objective is to compare (3.5)-(3.6) and determine which one is optimal. To do this, we enforce equal unicast rates of (3.5)-(3.6) and compare their broadcast rates. Specifically, hybrid capacity region (3.5) and (3.6) can be rewritten as:

$$C^1_{hybrid} = \{E[Blog_2(\frac{N_0B + P|h^b|^2}{N_0B + P^u_1|h^b|^2})], Blog_2(1 + \frac{P^u_1|h^u|^2}{N_0B})\} \tag{3.7}$$

$$C^2_{hybrid} = \{E[Blog_2(1 + \frac{P^b_2|h^b|^2}{N_0B})], Blog_2(1 + \frac{N_0B + P|h^u|^2}{N_0B + P^b_2|h^u|^2})\} \tag{3.8}$$

Let $R^u_1 = R^u_2$ in (3.7) and (3.8), we have:

$$P^b_2 = \frac{N_0B(P - P^u_1)}{N_0B + P^u_1|h^u|^2} \tag{3.9}$$

Plug (3.9) back in (3.7)-(3.8) and denote the same unicast rate as R^u, we have:

$$C^1_{hybrid} = \{E[\frac{B}{ln2}ln(\frac{N_0B + P|h^b|^2}{N_0B + P^u_1|h^b|^2})], R^u)\} \tag{3.10}$$

$$C^2_{hybrid} = \{E[\frac{B}{ln2}ln(1 + \frac{(P - P^u_1)|h^b|^2}{N_0B + P^u_1|h^u|^2})], R^u)\} \tag{3.11}$$

In order to determine the optimal DPC interference pre-cancellation order, we need to compare broadcast ergodic rates in (3.10)-(3.11), which depend on the distribution of h^b. Since broadcast network has many receivers, the common information transmission rate is determined by the receiver who has the worst channel statistics (usually at the coverage edge). Therefore, $|h^b|$ refers to the channel gain of the worst broadcast receiver. Similar to chapter 2, for broadcast channel, we can assume $|h^b|^2$

follows chi-squared distribution with mean $2\sigma^2$ where σ^2 is determined by equation (2.58)-(2.59).

According to the law of unconscious statistician, we can calculate the broadcast ergodic rates in (3.10)-(3.11) as:

$$\begin{aligned} E[ln(1+\frac{(P-P_1^u)|h^b|^2}{N_0B+P_1^u|h^u|^2})] &= \frac{1}{\sigma^2}\int_0^\infty ln(1+\frac{(P-P_1^u)x}{N_0B+P_1^u|h^u|^2})exp(-\frac{x}{\sigma^2})dx \\ &= exp[\frac{N_0B+P_1^u|h^u|^2}{(P-P_1^u)\sigma^2}]\Gamma(0,\frac{N_0B+P_1^u|h^u|^2}{(P-P_1^u)\sigma^2}) \end{aligned} \tag{3.12}$$

$$\begin{aligned} E[ln(\frac{N_0B+P|h^b|^2}{N_0B+P_1^u|h^b|^2})] &= E[ln(N_0B+P|h^b|^2)] - E[(N_0B+P_1^u|h^b|^2)] \\ &= exp[\frac{N_0B}{P\sigma^2}]\Gamma(0,\frac{N_0B}{P\sigma^2}) - exp[\frac{N_0B}{P_1^u\sigma^2}]\Gamma(0,\frac{N_0B}{P_1^u\sigma^2}) \end{aligned} \tag{3.13}$$

where $\Gamma(s,x)$ is the upper incomplete gamma function as defined in equation (2.16). Similarly, we denote $g(x) = exp(x)\Gamma(0,x)$ so $g(x)$ can be computed using (2.20).

Theorem 3.1. *For hybrid rate regions (3.5) and (3.6), the optimal interference pre-cancellation order is determined as:*

a) If $g(\frac{N_0B}{P\sigma^2}) > g(\frac{N_0B}{P^u\sigma^2}) + g(\frac{N_0B+P^u|h^u|^2}{P^b\sigma^2})$*, then the optimal DPC interference cancellation order is to cancel BC from UC.*

b) If $g(\frac{N_0B}{P\sigma^2}) < g(\frac{N_0B}{P^u\sigma^2}) + g(\frac{N_0B+P^u|h^u|^2}{P^b\sigma^2})$*, then the optimal DPC interference cancellation order is to cancel UC from BC.*

Proof. Subtract (3.12) from (3.13), we have:

$$g(\frac{N_0B}{P\sigma^2}) - g(\frac{N_0B}{P_1^u\sigma^2}) - g(\frac{N_0B+P_1^u|h^u|^2}{(P-P_1^u)\sigma^2}) \tag{3.14}$$

If equation (3.14) is greater than zero, according to our previous analysis, C_{hybrid}^1 is strictly higher than C_{hybrid}^2, so the optimal cancellation order is cancel BC from UC.

Similarly, the conclusion of part (b) is straightforward. Note that in the special case of:

$$g(\frac{N_0B}{P\sigma^2}) = g(\frac{N_0B}{P^u\sigma^2}) + g(\frac{N_0B + P^u|h^u|^2}{P^b\sigma^2}) \tag{3.15}$$

the two interference cancellation schemes are equivalent. □

For the general capacity region (3.1), there are more than one unicast users in the hybrid network. Without loss of generality, we assume $|h^u(1)| > |h^u(2)| > \cdots > |h^u(K)|$. Consider the broadcast ergodic rate in hybrid rate region (3.1), we have the following theorem:

Theorem 3.2. *In a hybrid network consisting of one broadcast signal and K unicast signals such that* $|h^u(1)| > |h^u(2)| > \cdots > |h^u(K)|$*, given power allocation* $P^b, P^u(1), P^u(2), , P^u(K)$*, the optimal DPC interference pre-cancellation order is determined as: Find the largest unicast user index* j $(1 \leq j \leq K)$ *such that:*

$$g[\frac{N_0B}{(P^b + \alpha_j)\sigma^2}] + g(\frac{N_0B}{\alpha_{j-1}\sigma^2}) > g(\frac{N_0B}{\alpha_j\sigma^2}) + g[\frac{N_0B}{(\alpha_{j-1} + \beta_j)\sigma^2}] \tag{3.16}$$

where $\alpha_j = \sum_{k=1}^{j} P^u(k)$*,* $\alpha_0 = 0$*, and* $\beta_j = \frac{N_0B+\alpha_{j-1}|h^u(j)|^2}{N_0B+\alpha_j|h^u(j)|^2}P^b$*. Then the optimal DPC interference cancelation order is* $UC(K) \rightarrow \cdots UC(j+1) \rightarrow BC \rightarrow UC(j) \cdots \rightarrow UC(1)$*, where "*$a \rightarrow b$*" indicates signal a is canceled from signal b.*

Proof. According to the results in [66], when the channel gains are known, the optimal DPC interference cancellation order is always to protect the signal with better channel condition and cancel those with smaller channel gain. According to Theorem 3.1, we can get the conclusion of Theorem 3.2. □

3.2.2. Hybrid network with multiple BCs

We have investigated the optimal DPC pre-cancellation among one broadcast signal and unicast signals. However, when the network consists of multiple broadcast

signals, the optimal DPC cancellation order is still unknown. For the convenience of discussion, we first assume that the network only consists of two broadcast signals. Without loss of generality, we denote the two broadcast signals as BC_1 and BC_2. Then the capacity region (3.1)-(3.2) become:

$$C_{hybrid} = [R^b(1), R^b(2)] \tag{3.17}$$

$$\mathbf{s.t.}: P^b(1) + P^b(2) = P \tag{3.18}$$

Using the similar idea as in single BC case, only two interference cancellation orders are possible: (1) BC_1 is pre-canceled from BC_2; (2) BC_2 is pre-canceled from BC_1. Thus we can write the achievable rate regions as:

$$C^1_{hybrid} = [R^b_1(1), R^b_1(2)] = \{E[Blog_2(\frac{N_0B + P|h^b(1)|^2}{N_0B + P^b_1|h^b(1)|^2})], E[Blog_2(1+\frac{P^b_1(2)|h^b(2)|^2}{N_0B})]\} \tag{3.19}$$

$$C^2_{hybrid} = [R^b_2(1), R^b_2(2)] = \{E[Blog_2(1+\frac{P^b_2(1)|h^b(1)|^2}{N_0B})], E[Blog_2(\frac{N_0B + P|h^b(2)|^2}{N_0B + P^b_2|h^b(2)|^2})]\} \tag{3.20}$$

where $R_i(j)$ $(i, j = 1, 2)$ indicates the rate of jth BC signal under the pre-cancellation order i and $P^b_i(j)$ $(i, j = 1, 2)$ indicates the power allocated to jth BC signal under the pre-cancellation order i. Also, $|h^b(1)|$, $|h^b(2)|$ are the channel gains of BC_1 and BC_2 and they are assumed to be Rayleigh distributed. Thus $|h^b(1)|^2$, $|h^b(2)|^2$ are chi-square distributed with expectations $\sigma^2(1)$ and $\sigma^2(2)$. Without loss of generality, we assume $\sigma^2(1) \geq \sigma^2(2)$. For $R^b_1(1)$ and $R^b_2(2)$, we can rewrite them as:

$$R^b_1(1) = R_0(1) - E[Blog_2(\frac{N_0B + P^b_1(2)|h^b(1)|^2}{N_0B})] \tag{3.21}$$

$$R^b_2(2) = R_0(2) - E[Blog_2(\frac{N_0B + P^b_2(1)|h^b(2)|^2}{N_0B})] \tag{3.22}$$

where $R_0(i) = E[Blog_2(\frac{N_0B+P|h^b(i)|^2}{N_0B})]$, $i = 1, 2$ are the rate of BC_1 and BC_2 when all power is allocated on it respectively. Thus, we have:

$$C^1_{hybrid} = \{R_0(1) - E[Blog_2(1 + \frac{P^b_1(2)|h^b(1)|^2}{N_0B})], E[Blog_2(1 + \frac{P^b_1(2)|h^b(2)|^2]}{N_0B})\} \quad (3.23)$$

$$C^2_{hybrid} = \{E[Blog_2(1 + \frac{P^b_2(1)|h^b(1)|^2}{N_0B}], R_0(2) - E[Blog_2(1 + \frac{P^b_2(1)|h^b(2)|^2}{N_0B})]\} \quad (3.24)$$

Theorem 3.3. *In low SNR condition, for two broadcast signals BC_1 and BC_2 such that $E[|h^b(1)|^2] \geq E[|h^b(2)|^2]$, the optimal DPC interference cancellation order between is to cancel BC_1 from BC_2.*

Proof. By calculation, we have:

$$R_0(1) = exp[\frac{N_0B}{P\sigma(1)^2}]\Gamma(0, \frac{N_0B}{P\sigma(1)^2}) = g[\frac{N_0B}{P\sigma(1)^2}] \quad (3.25)$$

$$R_0(2) = g[\frac{N_0B}{P\sigma(2)^2}] \quad (3.26)$$

$$E[Blog_2(\frac{N_0B + P^b_1(2)|h^b(1)|^2}{N_0B})] = g[\frac{N_0B}{P^b_1(2)\sigma(1)^2}] \quad (3.27)$$

$$E[Blog_2(\frac{N_0B + P^b_2(1)|h^b(1)|^2}{N_0B})] = g[\frac{N_0B}{P^b_2(1)\sigma(1)^2}] \quad (3.28)$$

$$E[Blog_2(\frac{N_0B + P^b_1(2)|h^b(2)|^2}{N_0B})] = g[\frac{N_0B}{P^b_1(2)\sigma(2)^2}] \quad (3.29)$$

$$E[Blog_2(\frac{N_0B + P^b_2(1)|h^b(2)|^2}{N_0B})] = g[\frac{N_0B}{P^b_2(1)\sigma(2)^2}] \quad (3.30)$$

Using similar idea, we enforce the first term of (3.23)-(3.24) to be equal and compare the second term. Thus, we have:

$$g[\frac{N_0B}{P\sigma(1)^2}] = g[\frac{N_0B}{P^b_1(2)\sigma(1)^2}] + g[\frac{N_0B}{P^b_2(1)\sigma(1)^2}] \quad (3.31)$$

In low SNR case, since the value of $\frac{P\sigma(i)^2}{N_0 B}$, $i = 1, 2$ are very small, which means $\frac{N_0 B}{P\sigma(i)^2}$ are very large. According to [69], for upper incomplete gamma function $g(x)$, when x is very large, we have following approximation:

$$g(x) = \frac{1}{x} + c_0 \tag{3.32}$$

where c_0 is a constant falling between 0.023 and 0.024. Thus, for equation (3.31), we have:

$$\frac{P - P_1^b(2) - P_2^b(1)}{N_0 B}\sigma(1)^2 = c_0 \tag{3.33}$$

Similarly, substract the second term of C_{hybrid}^1 from C_{hybrid}^2, we have

$$C_{hybrid}^2 - C_{hybrid}^1 = \{0, \frac{P - P_1^b(2) - P_2^b(1)}{N_0 B}\sigma(2)^2 - c_0\} \tag{3.34}$$

According to (43), since $c_0 > 0$, we have: $P - P_1^b(2) - P_2^b(1) > 0$. Thus, for $\sigma(2)^2 < \sigma(1)^2$, $\frac{P - P_1^b(2) - P_2^b(1)}{N_0 B}\sigma(2)^2 - c_0 < 0$. This indicates that C_{hybrid}^1 has larger capacity region. Thus the optimal cancellation should be BC_1 is cancelled from BC_2. □

Based on Theorem 3.3, in general, with M broadcast signals, we have the following corollary:

Corollary 3.1. *In low SNR condition, for M broadcast signals $BC_1, BC_2, , BC_M$ such that $E[|h^b(1)|^2] > E[|h^b(2)|^2] > \cdots > E[|h^b(M)|^2]$, the optimal DPC interference cancellation order is $BC_1 \to BC_2 \to \cdots \to BC_M$.*

Proof. If optimal DPC interference cancellation order is not $BC_1 \to BC_2 \to \cdots \to BC_M$. Then we assume for the optimal cancellation order is $BC_{t_1} \to BC_{t_2} \to \cdots \to BC_{t_M}$ where $t_1, t_2, \cdots, t_M$ is a permutation of $1, 2, \cdots, M$. Since $BC_1 \to BC_2 \to$

$\cdots \rightarrow BC_M$ is not the optimal cancellation order, then for $t_1, t_2, \cdots, t_M$, there exists t_i such that $t_i > t_{i+1}$.

Now consider another cancellation order $BC_{t_1} \rightarrow BC_{t_2} \rightarrow \cdots BC_{t_{i+1}} \rightarrow BC_{t_i} \cdots \rightarrow BC_{t_M}$. According to Theorem 3.3, $BC_{t_1} \rightarrow BC_{t_2} \rightarrow \cdots BC_{t_{i+1}} \rightarrow BC_{t_i} \cdots \rightarrow BC_{t_M}$ will have larger capacity region than $BC_{t_1} \rightarrow BC_{t_2} \rightarrow \cdots \rightarrow BC_{t_M}$ since $E[|h^b(i)|^2]E[|h^b(i+1)|^2]$. This violates the optimal cancellation order $BC_{t_1} \rightarrow BC_{t_2} \rightarrow \cdots \rightarrow BC_{t_M}$. Contradiction!

Thus, optimal DPC interference cancellation order is $BC_1 \rightarrow BC_2 \rightarrow \cdots \rightarrow BC_M$. □

Using Theorem 3.2 and Corollary 3.1, we can get the optimal cancellation order for a general hybrid network in low SNR:

Corollary 3.2. *In low SNR condition, for a general hybrid network consisting of M broadcast signals $BC_1, BC_2, \cdots, BC_M$ such that $E[|h^b(1)|^2] \geq E[|h^b(2)|^2] \geq \cdots \geq E[|h^b(M)|^2]$, and K unicast signals $UC_1, UC2, \cdots, UC_K$ such that $|h^u(1)| > |h^u(2)| > \ > |h^u(K)|$, then optimal DPC interference cancellation order is $BC_1 \rightarrow BC_2 \cdots \rightarrow BC_M \rightarrow UC(K) \rightarrow UC(K-1) \cdots \rightarrow UC(1)$*

Proof. In Theorem 3.2, the criteria for determining the cancellation order between BC and UC is:

$$g(\frac{N_0 B}{(P^b + \alpha_j)\sigma^2}) + g(\frac{N_0 B}{\alpha_{j-1}\sigma^2}) > g(\frac{N_0 B}{\alpha_j \sigma^2}) + g(\frac{N_0 B}{(\alpha_{j-1} + \beta_j)\sigma^2}) \tag{3.35}$$

According to (3.33), we have:

$$g(\frac{N_0 B}{(P^b + \alpha_j)\sigma^2}) + g(\frac{N_0 B}{\alpha_{j-1}\sigma^2}) = 2c_0 + \frac{P^b + \alpha_j + \alpha_{j-1}}{N_0 B}\sigma^2 \tag{3.36}$$

$$g(\frac{N_0 B}{\alpha_j \sigma^2}) + g(\frac{N_0 B}{(\alpha_{j-1} + \beta_j)\sigma^2}) = 2c_0 + \frac{\beta_j + \alpha_j + \alpha_{j-1}}{N_0 B}\sigma^2 \tag{3.37}$$

Since $\alpha_j = \sum_{k=1}^{j} P^u(k) > \alpha_{j-1}$, $\beta_j = \frac{N_0 B + \alpha_{j-1}|h^u(j)|^2}{N_0 B + \alpha_j |h^u(j)|^2} P^b < P^b$, the inequality (3.35) holds for each unicast user j. This means with low SNR condition, for each BC, it should always be canceled from UC. Thus, for each BC signal, the interference power from the UC is same. On the other hand, according to Corollary 3.1, we know the optimal cancellation among all BC is $BC_1 \to BC_2 \to \cdots \to BC_M$. Thus, the optimal cancellation order is $BC_1 \to BC_2 \cdots \to BC_M \to UC(K) \to UC(K-1) \cdots \to UC(1)$. □

3.3. Hybrid network with multicarrier transmission

In section 3.2, we have discussed the optimal DPC-precancellation order in single carrier network. However, in order to obtain higher transmission rate, multicarrier transmission (e.g. OFDM) has been widely used in most of the broadband transmissions systems (WLAN, 4G-LTE, DVB). Comparing to the single carrier network, multicarrier transmission supports broadband data transmission without complicated time-domain equalization. In this part, we will keep investigating the DPC-precancellation order in multicarrier scenario.

3.3.1. Hybrid network with single BC

Similar to the discussion in the single carrier case, if there are N subcarriers in total, then for any given power allocation scheme, we can define the ergodic capacity region as:

$$\begin{aligned} C(\overrightarrow{\mathbf{J}}) &= [R^b, R^u] \\ &= \{E[\sum_{i=1}^{N} B_n log_2(1 + \frac{P^b(i)|h^b(i)|^2}{N_0 B_n + P^u(i) j(i) |h^b(i)|^2})], \\ &\sum_{i=1}^{N} B_n log_2(1 + \frac{P^u(i)|h^u(i)|^2}{N_0 B_n + P^b(i)[1 - j(i)]|h^u(i)|^2})\} \end{aligned} \tag{3.38}$$

where $P^b(i)$, $P^u(i)$ are power allocated on ith broadcast and unicast subcarrier; $h^b(i)$, $h^u(i)$ are the channel gain on the ith broadcast and unicast subcarrier; $B_n = B/N$ is the bandwidth on each subcarrier; $\overrightarrow{\mathbf{J}} = [j(1), j(2), \cdots, j(N)]$ is the cancellation order vector which decides the cancellation order on each subcarrier.

Usually, in order to reduce the complexity of pre-coding steps, we assume the cancellation order is same among all subcarriers. Thus, there are two possible cancellation orders: 1) cancel BC from UC; 2) cancel UC from BC. These pre-cancellation orders correspond to the following two capacity regions respectively:

$$\begin{aligned} C^1_{hybrid} &= [R^b_1, R^u_1] \\ &= \{E[\sum_{i=1}^{N} B_n log_2(1 + \frac{P^b_1(i)|h^b(i)|^2}{N_0 B_n + P^u_1(i)|h^b(i)|^2})], \sum_{i=1}^{N} B_n log_2(1 + \frac{P^u_1(i)|h^u(i)|^2}{N_0 B_n})\} \end{aligned} \tag{3.39}$$

$$\begin{aligned} C^2_{hybrid} &= [R^b_2, R^u_2] \\ &= \{E[\sum_{i=1}^{N} B_n log_2(1 + \frac{P^b_2(i)|h^b(i)|^2}{N_0 B_n})], \sum_{i=1}^{N} B_n log_2(1 + \frac{P^u_2(i)|h^u(i)|^2}{N_0 B_n + P^b_2(i)|h^u(i)|^2})\} \end{aligned} \tag{3.40}$$

Thus, we can write R^b_1 and R^b_2 in forms of function $g(x)$ as:

$$R^b_1 = B_n \sum_{i=1}^{N} g[\frac{N_0 B_n}{P(i)\sigma(i)^2}] - B_n \sum_{i=1}^{N} g[\frac{N_0 B_n}{P^u_1(i)\sigma(i)^2}] \tag{3.41}$$

$$R^b_2 = B_n \sum_{i=1}^{N} g[\frac{N_0 B_n}{P^b_2(i)\sigma(i)^2}] \tag{3.42}$$

where $P(i)$ is the total power allocated on subcarrier i. In general,according to equation (3.41) and (3.42), when comparing C^1_{hybrid} with C^2_{hybrid}, we can let $R^u_1 = R^u_2$ and compare R^b_1 with R^b_2. Thus we have following theorem:

Theorem 3.4. *For hybrid rate region (3.39) and (3.40), the optimal interference pre-cancellation order is determined as:*

a) If $\sum_{i=1}^{N} g[\frac{N_0 B}{P(i)\sigma(i)^2}] > \sum_{i=1}^{N} g[\frac{N_0 B}{P^0(i)\sigma(i)^2}] + \sum_{i=1}^{N} g[\frac{N_0 B}{P^b(i)\sigma(i)^2}]$*, then the optimal DPC interference cancellation order is to cancel BC from UC,*

b) If $\sum_{i=1}^{N} g[\frac{N_0 B}{P(i)\sigma(i)^2}] < \sum_{i=1}^{N} g[\frac{N_0 B}{P^0(i)\sigma(i)^2}] + \sum_{i=1}^{N} g[\frac{N_0 B}{P^b(i)\sigma(i)^2}]$*, then the optimal DPC interference cancellation order is to cancel UC from BC,*

where $P(i)$ *is the total power allocated to subcarrier* i *and* $P^b(i)$ *is the power allocated to broadcast on subcarrieri. Moreover,* $P^0(1), P^0(2), \cdots, P^0(N)$ *is the solution of the following equation:*

$$\prod_{i=1}^{N}(1+\frac{P^0(i)|h^u(i)|^2}{N_0 B_n}) = \prod_{i=1}^{N}\frac{N_0 B_n + P(i)|h^u(i)|^2}{N_0 B_n + P^b(i)|h^u(i)|^2} \tag{3.43}$$

Proof. When $R_1^u = R_2^u$, we have:

$$\prod_{i=1}^{N}(1+\frac{P_1^u(i)|h^u(i)|^2}{N_0 B_n}) = \prod_{i=1}^{N}\frac{N_0 B_n + P(i)|h^u(i)|^2}{N_0 B_n + P_2^b(i)|h^u(i)|^2} \tag{3.44}$$

Thus, if $[P^0(1), P^0(2), \cdots, P^0(N)]$ is the solution of (3.43), it corresponds to one power allocation that reaches same unicast rate in C_{hybrid}. Subtract (3.41) from (3.42), we have:

$$g(\frac{N_0 B}{P\sigma^2}) - g(\frac{N_0 B}{P_1^u\sigma^2}) - g(\frac{N_0 B + P_1^u|h^u|^2}{(P-P_1^u)\sigma^2}) \tag{3.45}$$

If equation (3.45) is greater than zero, according to our previous analysis,C_{hybrid}^1 is strictly higher than C_{hybrid}^2, so the optimal cancellation order is cancel BC from UC. Similarly, the conclusion of part (b) is straightforward using same method. □

For Theorem 3.4, it is still not easy to determine the pre-cancellation order since $g(x)$ is difficult to compute. However, in low SNR condition, by applying

approximation to $g(x)$, the DPC-cancellation order can be determined by following theorem:

Theorem 3.5. *In low SNR condition, a hybrid network consisting of one BC and one UC, the optimal DPC cancellation order is to cancel BC from UC.*

Proof. According to (3.33), in low SNR condition, we have:

$$R_1^b = \sum_{i=1}^{N} \frac{[P(i) - P_1^u(i)]\sigma(i)^2}{N_0} \tag{3.46}$$

$$R_2^b = Bc_0 + \sum_{i=1}^{N} \frac{P_2^b(i)\sigma(i)^2}{N_0} \tag{3.47}$$

On the other hand, we can approximate $ln(1+x)$ as x when x is small. Thus, in low SNR condition:

$$R_1^u = \sum_{i=1}^{N} \frac{P_1^u(i)|h^u(i)|^2}{N_0} \tag{3.48}$$

$$R_2^u = \frac{1}{N_0 ln2} \sum_{i=1}^{N} \frac{[P(i) - P_2^b(i)]|h^u(i)|^2}{1 + P_2^b(i)|h^u(i)|^2/N_0 B_n} \tag{3.49}$$

By letting $R_1^b = R_2^b$ and compare the second terms of C_{hybrid}^1, C_{hybrid}^2, we have:

$$Nc_0 = \sum_{i=1}^{N} \frac{[P(i) - P_1^u(i) - P_2^b(i)]\sigma(i)^2}{N_0 B_n} \tag{3.50}$$

In order to compare R_1^u with R_2^u, we consider their difference:

$$
\begin{aligned}
R_1^u - R_2^u &= \frac{1}{N_0 ln2} \sum_{i=1}^{N} \{P_1^u(i)|h^u(i)|^2 - \frac{[P(i) - P_2^b(i)]|h^u(i)|^2}{1 + P_2^b(i)|h^u(i)|^2/N_0 B_n}\} \\
&= \frac{1}{N_0 ln2} \sum_{i=1}^{N} \frac{[P_2^b(i) + P_1^u(i) - P(i)]|h^u(i)|^2 + P_1^u(i)|h^u(i)|^2 P_2^b(i)|h^u(i)|^2/N_0 B_n}{1 + P_2^b(i)|h^u(i)|^2/N_0 B_n} \\
&= \frac{1}{N_0 ln2} \sum_{i=1}^{N} \frac{[2max(P_1^u(i), P_2^b(i)) - P(i)]|h^u(i)|^2}{1 + max(P_2^b(i), P_1^u(i))|h^u(i)|^2/N_0 B_n}
\end{aligned}
\tag{3.51}
$$

since $2max(P_1^u(i), P_2^b(i)) - P(i) > 0$, we have $R_1^u > R_2^u$. Thus, C_{hybrid}^1 is larger than C_{hybrid}^2, which means that canceling BC from UC can get larger capacity region. □

According to Theorem 3.5, in low SNR condition, the optimal DPC pre-cancellation order is always cancel BC from UC. However, with different power allocation scheme, we can reach different point in capacity region. In order to obtain the boundary of capacity region, for any given pair (μ_1, μ_2) such that $0 \leq \mu_1, \mu_2 \leq 1$, our goal is to maximize the $\mu_1 R^b + \mu_2 R^u$. Since in low SNR condition, based on equation (2.21), we have:

$$
R^b = \sum_{n=1}^{N} \frac{B_n}{ln2} (\frac{|h_n^b|^2 P_n^b}{N_0 B_n + |h_n^b|^2 P_n^u}) \tag{3.52}
$$

Meanwhile, due to the DPC pre-cancellation order, we have the unicast rate as:

$$
R^u = \sum_{n=1}^{N} \frac{B_n}{ln2} ln(1 + \frac{|h_n^u|^2 P_n^u}{N_0 B_n}) \tag{3.53}
$$

Thus, in order to optimize $\mu_1 R^b + \mu_2 R^u$, it is equivalent to following problem:

$$
\underset{\overrightarrow{p}=(P_1, P_2, \cdots, Pn)}{max} \{\mu_1 \sum_{n=1}^{N} \frac{|h_n^b|^2 P_n^b}{N_0 B_n + |h_n^b|^2 P_n^u} + \mu_2 \sum_{n=1}^{N} ln(N_0 B_n + |h_n^u|^2 P_n^u)\} \tag{3.54}
$$

$$s.t.: \sum_{i=1}^{N}(P_n^u + P_n^b) = P \tag{3.55}$$

According to Theorem 2.1, the first term of (3.54) gets its maximum value when the power in broadcast network allocated inversely:

$$P_n^b = \frac{\frac{1}{\sigma_i^2}}{\sum_{i=1}^{N}\frac{1}{\sigma_i^2}} \quad n = 1, 2, \cdots, N \tag{3.56}$$

where the $\sigma_i^2 = E[|h_i^u|^2]$.On the other hand, using method of least square for (3.54), we have the following condition when it reaches its maximum:

$$N_0 B_n + |h_n^u|^2 P_n^u = \frac{\mu_1}{\mu_2 \sum_{i=1}^{N}\frac{1}{\sigma_i^2}} P^b \quad n = 1, 2, \cdots, N \tag{3.57}$$

From (3.56) and (3.57), we can see that the capacity region reaches its maximum value when the broadcast power are located inversely proportional to the variance of each subcarrier while using the water-filling power allocation scheme in the unicast network. Furthermore, we can get the relationship between the P^b and P^u as:

$$P^b = \frac{P + N_0 B_n \sum_{i=1}^{N}\frac{1}{|h_i^u|^2}}{1 + \frac{\mu_1 \sum_{i=1}^{N}\frac{1}{|h_i^u|^2}}{\mu_2 \sum_{i=1}^{N}\frac{1}{\sigma_i^2}}} \tag{3.58}$$

$$P^u = \frac{P\frac{\mu_1 \sum_{i=1}^{N}\frac{1}{|h_i^u|^2}}{\mu_2 \sum_{i=1}^{N}\frac{1}{\sigma_i^2}} - N_0 B_n \sum_{i=1}^{N}\frac{1}{|h_i^u|^2}}{1 + \frac{\mu_1 \sum_{i=1}^{N}\frac{1}{|h_i^u|^2}}{\mu_2 \sum_{i=1}^{N}\frac{1}{\sigma_i^2}}} \tag{3.59}$$

In fact, when the power is optimally allocated, we can infer from the (3.58) and (3.59) that $N_0 B_n + |h_n^u|^2 p_n^u + P_n^b \sigma_n^2$ are equal on each subcarrier. This is analogous to the traditional water-filling on unicast only. We call this as "double water-filling".

Using same approach, in general, if we have M broadcast networks in a hybrid network, we can generalize the (3.54) as:

$$\mu_0 \sum_{i=1}^{N} ln(N_0 B_n + |h_i^u|^2 P_i^u) + \mu_1 \sum_{i=1}^{N} \frac{|h_i^1|^2 P_i^1}{N_0 B_n + |h_i^1|^2 P_i^u} + \mu_2 \sum_{i=1}^{N} \frac{|h_i^2|^2 P_i^2}{N_0 B_n + |h_i^2|^2 P_i^1 + |h_i^2|^2 P_i^u} + \cdots + \mu_M \sum_{i=1}^{N} \frac{|h_n^M|^2 P_i^M}{N_0 B_n + \sum_{k=1}^{M-1} |h_i^M|^2 P_i^k + |h_n^M|^2 P_i^u} \tag{3.60}$$

Here we assume $|h_n^1|^2 \leq |h_n^2|^2 \leq \cdots \leq |h_n^M|^2$, and $0 \leq \mu_0, \mu_1, \cdots, \mu_M \leq 1$. Notice for any two neighboring terms in (3.60), they have the similar form as (3.54). We can get the following optimal power allocation scheme:

$$P_n^i = \frac{P(\frac{1}{\mu_i} \sum_{j=1}^{N} \frac{1}{\sigma_{ij}^2}) + N_0 B_n \sum_{j=1}^{N} \frac{1}{|h_j^u|^2} (\frac{1}{\mu_i} \sum_{j=1}^{N} \frac{1}{\sigma_{ij}^2})}{\frac{1}{\mu_0} \sum_{j=1}^{N} \frac{1}{|h_j^u|^2} + \frac{1}{\mu_1} \sum_{j=1}^{N} \frac{1}{\sigma_{1j}^2} + \cdots + \frac{1}{\mu_M} \sum_{j=1}^{N} \frac{1}{\sigma_{Mj}^2}} \quad i = 1, 2, \cdots, M \tag{3.61}$$

$$P_n^i = \frac{P(\frac{1}{\mu_i} \sum_{j=1}^{N} \frac{1}{|h_j^u|^2}) - N_0 B_n \sum_{j=1}^{N} \frac{1}{|h_j^u|^2} \sum_{k=1}^{M} (\frac{1}{\mu_k} \sum_{j=1}^{N} \frac{1}{\sigma_{kj}^2})}{\frac{1}{\mu_0} \sum_{j=1}^{N} \frac{1}{|h_j^u|^2} + \frac{1}{\mu_1} \sum_{j=1}^{N} \frac{1}{\sigma_{1j}^2} + \cdots + \frac{1}{\mu_M} \sum_{j=1}^{N} \frac{1}{\sigma_{Mj}^2}} \quad n = 1, 2, \cdots, N \tag{3.62}$$

Thus, equation (3.61) and (3.62) give the optimal power allocation scheme for low SNR condition.

3.3.2. Hybrid network with multiple BCs

For the multicarrier hybrid network consisting of two BC signals, the capacity region $C(\overrightarrow{\mathbf{J}}) = [R^{b_1}, R^{b_2}]$ can be represented as the following form:

$$
\begin{aligned}
C(\overrightarrow{\mathbf{J}}) &= [R^{b_1}, R^{b_2}] \\
&= \{E[\sum_{i=1}^{N} B_n log_2(1 + \frac{P^{b_1}(i)|h^{b_1}(i)|^2}{N_0 B_n + P^{b_2}(i) j(i) |h^{b_1}(i)|^2})], \\
&\sum_{i=1}^{N} B_n log_2(1 + \frac{P^{b_2}(i)|h^{b_2}(i)|^2}{N_0 B_n + P^{b_1}(i)[1 - j(i)]|h^{b_2}(i)|^2})\}
\end{aligned} \tag{3.63}
$$

where $P^{b_1}(i)$, $P^{b_2}(i)$ are power allocated on ith broadcast and unicast subcarrier; $h^{b_1}(i)$, $h^{b_2}(i)$ are the broadcast channel gain on the ith broadcast subcarrier. $\overrightarrow{\mathbf{J}} = [j(1), j(2), \cdots, j(N)]$ is the cancellation order vector which decides the cancellation order on each subcarrier.

Similar to section 3.3.1, for convenience of our discussion, we assume the cancellation order is same among all subcarriers. Thus, with different cancellation order, we have:

$$
\begin{aligned}
C^1_{hybrid} &= [R^{b_1}_1, R^{b_2}_1] \\
&= \{E[\sum_{i=1}^{N} B_n log_2(1 + \frac{P^{b_1}_1(i)|h^{b_1}(i)|^2}{N_0 B_n + P^{b_2}_1(i)|h^{b_1}(i)|^2})], E[\sum_{i=1}^{N} B_n log_2(1 + \frac{P^{b_2}_1(i)|h^{b_2}(i)|^2}{N_0 B_n})]\}
\end{aligned} \tag{3.64}
$$

$$
\begin{aligned}
C^2_{hybrid} &= [R^{b_1}_2, R^{b_2}_2] \\
&= \{E[\sum_{i=1}^{N} B_n log_2(1 + \frac{P^{b_1}_2(i)|h^{b_1}(i)|^2}{N_0 B_n})], E[\sum_{i=1}^{N} B_n log_2(1 + \frac{P^{b_2}_2(i)|h^{b_2}(i)|^2}{N_0 B_n + P^{b_1}_2(i)|h^{b_2}(i)|^2})]\}
\end{aligned} \tag{3.65}
$$

By calculation, we have:

$$
R^{b_1}_1 = B_n \sum_{i=1}^{N} g[\frac{N_0 B_n}{P(i)\sigma_1(i)^2}] - B_n \sum_{i=1}^{N} g[\frac{N_0 B_n}{P^{b_2}_1(i)\sigma_1(i)^2}] \tag{3.66}
$$

$$R_1^{b_2} = B_n \sum_{i=1}^{N} g[\frac{N_0 B_n}{P_1^{b_2}(i)\sigma_2(i)^2}] \tag{3.67}$$

$$R_2^{b_1} = B_n \sum_{i=1}^{N} g[\frac{N_0 B_n}{P_2^{b_1}(i)\sigma_1(i)^2}] \tag{3.68}$$

$$R_2^{b_2} = B_n \sum_{i=1}^{N} g[\frac{N_0 B_n}{P(i)\sigma_2(i)^2}] - B_n \sum_{i=1}^{N} g[\frac{N_0 B_n}{P_2^{b_1}(i)\sigma_2(i)^2}] \tag{3.69}$$

Using the same idea as Theorem 3.4, we have the following corollary to determine the DPC-cancellation order for two BCs in general:

Corollary 3.3. *For hybrid rate region (3.64) and (3.65) in general SNR condition, the optimal interference pre-cancellation order is determined as follow:*

a) If $\sum_{i=1}^{N} g[\frac{N_0 B_n}{P(i)\sigma_1(i)^2}] > \sum_{i=1}^{N} g[\frac{N_0 B_n}{P^{b_2}(i)\sigma_1(i)^2}] + \sum_{i=1}^{N} g[\frac{N_0 B_n}{P^0(i)\sigma_1(i)^2}]$*, then the optimal DPC interference cancellation order is to cancel BC1 from BC2,*

b) If $\sum_{i=1}^{N} g[\frac{N_0 B_n}{P(i)\sigma_1(i)^2}] < \sum_{i=1}^{N} g[\frac{N_0 B_n}{P^{b_2}(i)\sigma_1(i)^2}] + \sum_{i=1}^{N} g[\frac{N_0 B_n}{P^0(i)\sigma_1(i)^2}]$*, then the optimal DPC interference cancellation order is to cancel BC2 from BC1,*

where $P(i)$ *is the total power allocated to subcarrier* i *and* $P^{b_2}(i)$ *is the power allocated to* BC_2 *on subcarrier* i*. Moreover,* $P^0(1), P^0(2), \cdots, P^0(N)$ *is the solution of the following equation:*

$$\sum_{i=1}^{N} g[\frac{N_0 B_n}{P(i)\sigma_2(i)^2}] = \sum_{i=1}^{N} g[\frac{N_0 B_n}{P^{b_2}(i)\sigma_2(i)^2}] + \sum_{i=1}^{N} g[\frac{N_0 B_n}{P^0(i)\sigma_2(i)^2}] \tag{3.70}$$

3.4. DPC operation for outage capacity

As defined in chapter 2, when outage capacity is used for broadcast, the hybrid achievable rate region C_{hybrid}^1 and C_{hybrid}^2 becomes:

$$C_{hybrid}^1 = [R_1^b, R_1^u] = \{R_1^b, Blog_2(1 + \frac{P_1^u |h^u|^2}{N_0 B})\} \tag{3.71}$$

$$s.t. : Prob[Y_1 \leq R_1^b] = q^0 \tag{3.72}$$

$$C^2_{hybrid} = [R^b_2, R^u_2] = \{R^b_2, Blog_2(1 + \frac{P^u_2|h^u|^2}{N_0B + P^b_2|h^u|^2})\} \tag{3.73}$$

$$s.t. : Prob[Y_2 \leq R^b_2] = q^0 \tag{3.74}$$

where q^0 is the maximum broadcast outage probability, Y_1 and Y_2 are random variables given by:

$$Y_1 = Blog_2(\frac{N_0B + P|h^b|^2}{N_0B + P^u_1|h^b|^2}) \tag{3.75}$$

$$Y_2 = Blog_2(1 + \frac{P^b_2|h^b|^2}{N_0B}) \tag{3.76}$$

According to Theorem 1 in [66], it has been shown that the optimal DPC interference cancellation order is to cancel broadcast from unicast when $|h^T| \leq |h^u|$, where $Prob[|h^b| \leq |h^T|] = q^0$. To derive the general optimal DPC operation for Rayleigh fading channel, we need to first obtain the cumulative density function (CDF) for Y_1 and Y_2. The CDF of Y_1 can be expressed as:

$$F(Y_1 \leq y_0) = F[|h^b|^2 \leq \frac{N_0B(2^{\frac{y_0}{B}} - 1)}{P - 2^{\frac{y_0}{B}}P^u_1}] \tag{3.77}$$

Since $|h^b|^2$ follows chi-squared distribution with means σ^2, we have:

$$F(Y_1 \leq y_0) = \frac{1}{\sigma^2}\int_0^{\frac{N_0B(2^{\frac{y_0}{B}}-1)}{P-2^{\frac{y_0}{B}}P^u_1}} exp(-\frac{x}{\sigma^2})dx = 1 - exp[-\frac{N_0B(2^{\frac{y_0}{B}} - 1)}{P - 2^{\sigma^2(\frac{y_0}{B}}P^u_1)}] \tag{3.78}$$

Take equation (3.78) into (3.72), we have:

$$-\frac{N_0B(2^{\frac{R^b_1}{B}} - 1)}{\sigma^2(P - 2^{\frac{R^b_1}{B}}P^u_1)} = ln(1 - q^0) \tag{3.79}$$

Thus we get the expression of R_1^b:

$$R_1^b = Blog_2[1 - \frac{\sigma^2(P - P_1^u)ln(1-q^0)}{N_0B - \sigma^2 P_1^u ln(1-q^0)}] \tag{3.80}$$

Similarly, R_2^b can be expressed as:

$$R_2^b = Blog_2[1 - \frac{\sigma^2 P_2^b}{N_0B} ln(1-q^0)] \tag{3.81}$$

Compare equation (3.80) with (3.81), we have the following theorem:

Theorem 3.6. *For hybrid rate regions (3.71) and (3.73), the optimal DPC interference cancellation order is determined as:*

a) If $|h^u|^2 + \sigma^2 ln(1-q^0) > 0$, then the optimal DPC interference cancellation order is to cancel BC from UC.

b) If $|h^u|^2 + \sigma^2 ln(1-q^0) < 0$, then the optimal DPC interference cancellation order is to cancel UC from BC.

Proof. Using similar idea as the proof in Theorem 3.1, we enforce the same unicast rate in (3.71) and (3.73), then we compare the broadcast rates. Since R_1^u and R_2^u has the same expression as in (3.5) and (3.6), the relationship in (3.9) still holds and we plug it into (3.81) to get:

$$R_2^b = Blog_2[1 - \frac{\sigma^2(P - P_1^u)}{N_0B + P_1^u|h^u|^2} ln(1-q^0)] \tag{3.82}$$

Compare (3.82) with (3.80), and notice that $ln(1-q^0) \leq 0$, we have:

$$R_1^b \geq R_2^b \Longleftrightarrow |h^u|^2 + \sigma^2 ln(1-q^0) \geq 0 \tag{3.83}$$

Under this condition, the achievable rates of C^1_{hybrid} is strictly larger than C^2_{hybrid}. Thus, a) is proved. In a similar way we can prove b). □

Unlike Theorem 3.1, when consider broadcast outage rate, Theorem 3.6 indicates that the optimal interference cancellation order is independent of power allocation between the broadcast and unicast. For outage broadcast rate, according to [13], we can extend Theorem 3.6 to general hybrid network as follows:

Corollary 3.4. *In a hybrid network consisting of one broadcast signals and K unicast signals. If channel gains satisfy $|h^u(1)|^2 > |h^u(2)|^2 > \cdots > |h^u(i)|^2 > -\sigma^2 ln(1-q^0) > |h^u(i+1)|^2 > \cdots > |h^u(K)|^2$, the optimal DPC cancellation order is: $UC_K \rightarrow \cdots \rightarrow UC_{i+1} \rightarrow BC \rightarrow UC_i \rightarrow \cdots \rightarrow UC_1$, where σ^2 is the expectation of $|h^b|^2$, and q^0 is the broadcast outage probability.*

Proof. Accoring to [66], since $|h^u(1)|^2 > |h^u(2)|^2 > \cdots > |h^u(i)|^2 > |h^u(i+1)|^2 > \cdots > |h^u(K)|^2$, we know the optimal cancellation order among unicast signals is $UC_K \rightarrow \cdots \rightarrow UC_{i+1} \rightarrow UC_i \rightarrow \cdots \rightarrow UC_1$. For broadcast signal, according to Theorem 3.6, since $-\sigma^2 ln(1-q^0) > |h^u(i+1)|^2 > \cdots > |h^u(K)|^2$, $UC_K, \cdots UC_{i+1}$ should be canceled from BC. Similarly, BC should be canceled from $UC_1, \cdots UC_i$. Thus, the optimal cancellation order is $UC_K \rightarrow \cdots \rightarrow UC_{i+1} \rightarrow BC \rightarrow UC_i \rightarrow \cdots \rightarrow UC_1$. □

3.5. Simulation and discussion on results

For the convenience of illustration, all the simulation results in this section are based on one unicast signal and one or two broadcast signals such that we can plot the hybrid rate region in a two dimensional plane. We normalize the total power P and the average broadcast power gain σ^2 to be one. Using time division multiplexing (TDM) as the benchmark, Figure 3.2 provide the hybrid rate regions of different DPC schemes with broadcast ergodic capacity. In high SNR regime (SNR=10 dB),

Figure 3.2 shows that canceling BC in DPC yields larger capacity region for $|h^u|^2 = 3$. However, as $|h^u|^2$ decreases, the performance of canceling unicast in DPC gradually outperforms the other DPC scheme.

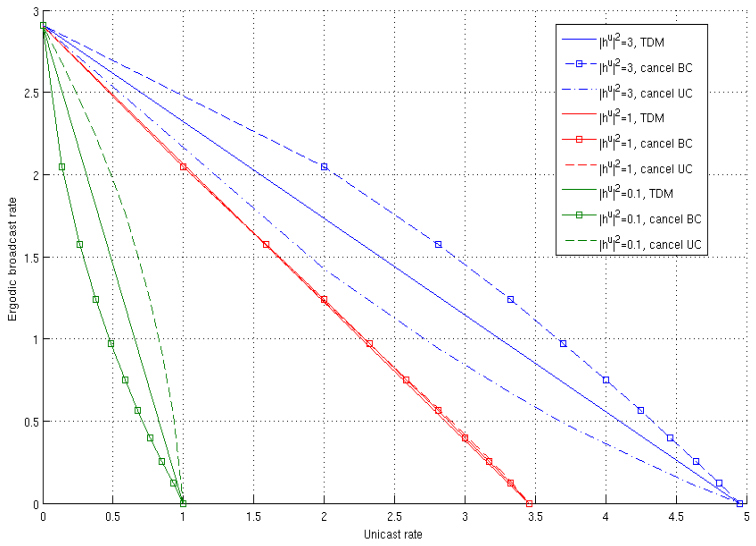

Figure 3.2. Ergodic hybrid rate region in high SNR condition

The hybrid rate regions in low SNR regime is presented in Figure 3.3 (SNR = -10 dB). We can see that the capacity region of either DPC canceling order is very close to the TDM. This is because the noise is dominant in low SNR so that the interference between BC and UC becomes trivial. In fact, the unicast rate in low SNR can be approximated as $log_2(1 + \frac{P_1^u|h^u|^2}{N_0 B}) = \frac{(P_1^u|h^u|^2}{N_0 B}$, thus the relationship between BC rate and UC rate is approximately linear.

In Figure 3.4, we consider moderate SNR regime by setting SNR=1.76 dB. We can see that both DPC rate regions are bigger than that of TDM. When $|h^u|^2 = 3$, the two DPC curves have an intersection at (1.7, 0.38). That is, when BC rate is greater than 0.38, canceling BC gives a larger rate region. Otherwise, when UC rate is greater than 1.7, canceling UC becomes the better DPC scheme. While in the case of $|h^u|^2 = 1$, two DPC schemes have almost the same rate region.

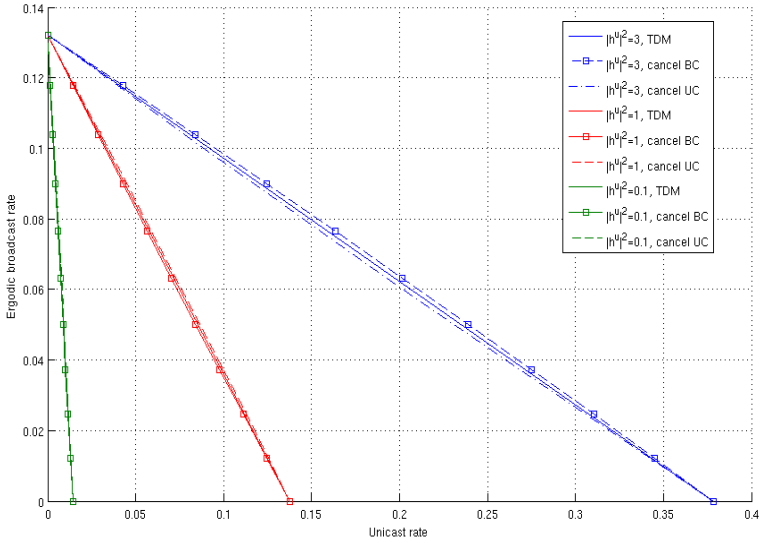

Figure 3.3. Ergodic hybrid rate region in low SNR condition

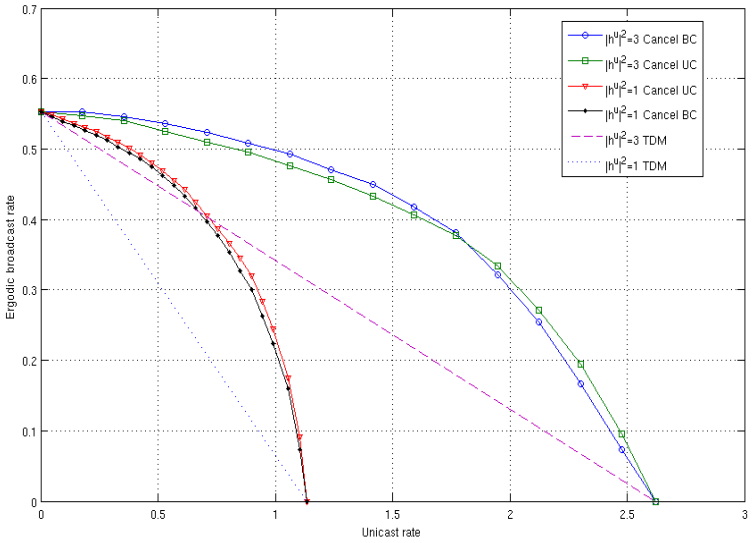

Figure 3.4. Ergodic hybrid rate region in moderate SNR

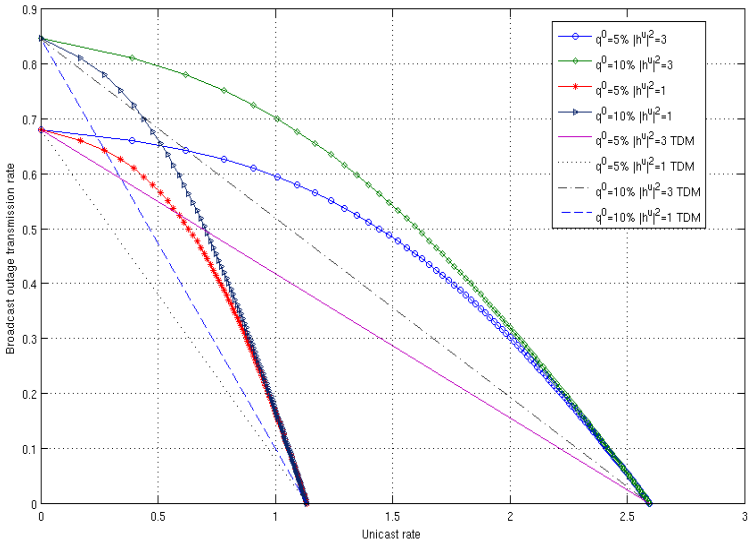

Figure 3.5. Outage hybrid rate region in moderate SNR

For the hybrid rate region with broadcast outage rate, according to Theorem 3.6, the optimal cancellation order is always to cancel BC signal from UC signal. We present the simulation results under the same moderate SNR=1.76 dB in Figure 3.5. Comparing with Figure 3.4, we can see that by allowing more outage, the capacity region can be extended

In Figure 3.6 and 3.7, we have showed the ergodic capacity region of two broadcast signals under different pre-cancellation order in low and moderate SNR conditions. In our simulation, we let $\sigma_1(i)^2 = 0.34$ and $\sigma_2(i)^2 = 0.06$. In Figure 3.6, we can see that cancel BC1 can always get a larger rate region than canceling BC2. Since $\sigma_1(i)^2 > \sigma_2(i)^2$, this matches to our conclusion in Theorem 3.3. In Figure 3.7 for multicarrier transmission case, the intersection is at (0.51, 0.58). This means in when BC2s rate is greater than 0.58, canceling BC1 will give larger rate region. Otherwise, canceling BC1 becomes better DPC scheme. Moreover, by comparing the case of multicarrier transmission, we can see that by adopting multicarrier transmission, the ergodic capacity is increased.

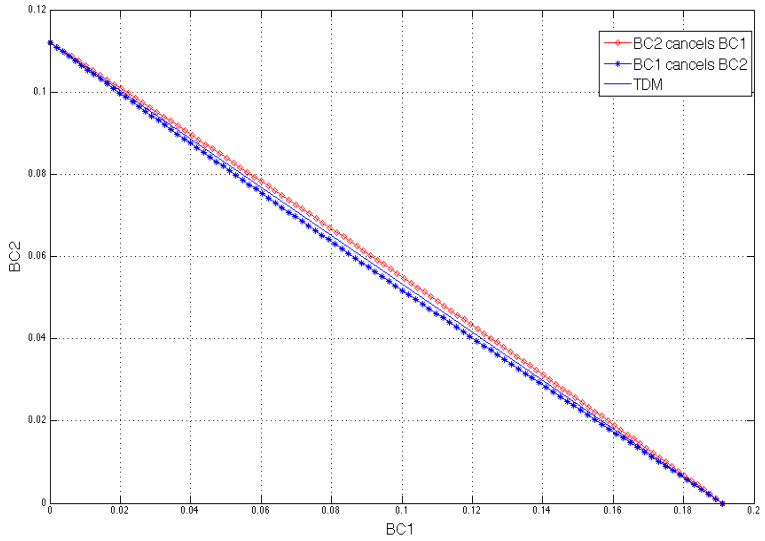

Figure 3.6. Ergodic hybrid rate region of two broadcasts in low SNR

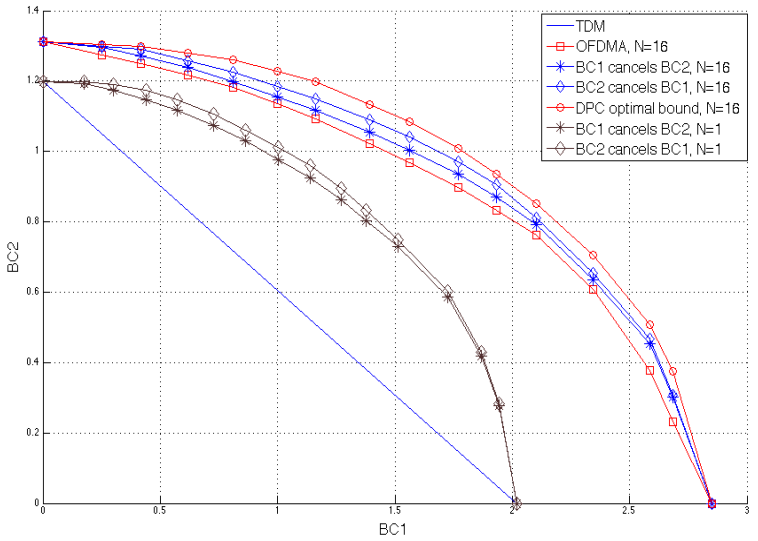

Figure 3.7. Ergodic hybrid rate region of two broadcasts in moderate SNR

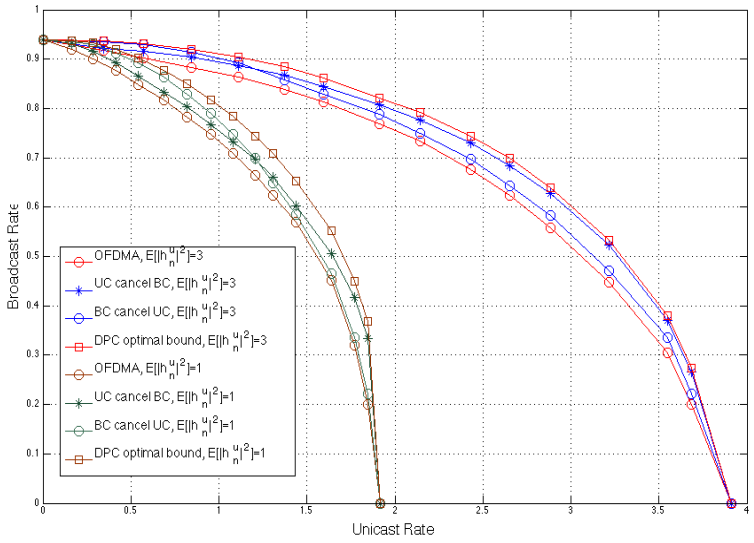

Figure 3.8. Ergodic hybrid BC/UC rate region in moderate SNR ($N = 16$)

Figure 3.8 shows the capacity region of a hybrid BC/UC system with multiple subcarriers. From the figure, we can see that when $|h^u|^2 = 3$, the two curves intersects at point very close to the endpoint of the curve. This means unless BCs rate is very high, otherwise, canceling BC can always obtain a larger rate region. On the other hand, when $|h^u|^2 = 1$, two curves intersects at (1.3, 0.7) which means when BC rate is greater than 0.7, canceling UC become the better DPC scheme. Also, by comparing Figure 3.8 with Figure 3.4, we can that by applying multicarrier transmission, we can get larger capacity region. On the other hand, we can see by adopting the multicarrier transmission, a larger capacity region is obtained. Moreover, the optimal capacity region is still reached when BC is pre-canceled from UC for most of the time, which coincides to the results in Theorem 3.5.

3.6. Summary

In this chapter, we considered the DPC-based broadcast and unicast cancellation order to get the best achievable rate region. We use both ergodic capacity and outage capacity to evaluate the broadcast performance. For both cases, we analytically

derived the conditions for optimal DPC operation. Furthermore, we extend our results to the multicarrier system and we present the criteria to determine the optimal DPC cancellation order. Finally, simulation results are provided to validate the analysis and gain important insights on the optimal DPC operation.

CHAPTER 4. CONCLUSIONS AND FUTURE WORK

This thesis presents two independent pieces of work: multicarrier broadcast coverage analysis and optimal capacity region of broadcast-unicast hybrid network. In Chapter 2, we studied multicarrier broadcast coverage area for SISO and MIMO system respectively. We provide statistical approximation and bounds for IMI which determined the broadcast area. More importantly, we provide the optimal power allocation schemes among subcarriers in low SNR and high SNR cases to reach the largest broadcast coverage. The performance gap between the optimal solution and our computation-efficient approximation becomes almost negligible with the increase in number of subcarriers. Our results also proves that by applying multicarrier joint-coding transmission scheme, the performance enhancement is significant and our power allocation schemes are always optimal in low and high SNR scenario. However, for the optimal power allocation in general, it is still unknown yet and we would like to find an adequate algorithm in future.

In hybrid network study, we discussed the interference precancellation order of a DPC-based collaborative broadcast and unicast network. In chapter 3, the optimal DPC-precancellation order is derived for a single-carrier transmission hybrid network. Then we extend our analysis to a practical hybrid system which deploying multicarrier transmission. We also derive the optimal power allocation algorithm that approach the hybrid capacity. Our results show that interference cancellation order is not fixed in general. With different power allocation scheme and various SNR condition, the optimal DPC precancellation order is changing all the time and can be determined by the criterion provided. however, in some special scenario such as low SNR environment, the DPC precancellation order can be solely determined. Future work on hybrid network includes but not limited to:

- Outage capacity with joint coding, where information bits are coded across both time slots and subcarriers. Actually, joint coding leads to a much higher capacity. However, due to the computation complexity, most of the discussion on outage capacity are still based on independent coding.

- Cross-layer hybrid network optimization. To realize true network convergence, it requires a bottom-up reconsideration of layer 1, 2 and associated network issues.

- The application of the DPC in wireless coexistence, where becomes a major in current 2.4GHz. Since both Wifi and bluetooth signal are occupying this band, the current solution is still based on TDM to reduce interference. Dirty paper coding provides a new path to achieve the wireless coexistence in the future.

REFERENCES

[1] Z. Hu and H. Liu, "A Low-Complexity Decoding Algorithm for Hierarchical Broadcasting: Design and Implementation", *IEEE Trans. on Vehicular Technology,* Vol. 2, Issue: 62, 2013.

[2] Z. Hu and H. Liu, "Structure-based Decoding for Hierarchically Modulated, LDPC coded Signals", *IEEE GLOBECOM'12,* California, USA, 3-7 Dec., 2012.

[3] Z. Hu, X. Shao, Z. Chen, G. Xing and H. Liu,"System Design for Broadband Digital Radio Broadcasting", *IEEE Communication Magazine,* Apr., 2013.

[4] Cisco, *Cisco Visual Networking Index: Global Mobile Data Traffic Forecast Update, 2012-2017*, Cisco, 2013.

[5] RNCOS Industry Research Solutions, *Global Mobile TV Forecast to 2013*, Aug., 2011.

[6] L. Dai, Z. Wang, Z. Yang, "Next-generation digital television terrestrial broadcasting systems: Key technologies and research trends", *IEEE Communications Magazine*, Vol. 50, Issue: 6, 2012.

[7] A. Chloe, "Introducation of the Multimedia Broadcast Multicast Service (MBMS) in the Radio Access Network (Rel.7 and 8)", *3GPP TS 25.346*, Dec., 2007.

[8] A. Chloe, "Verizon Eyes Broadcast Over LTE for Super Bowl 2014", *PC Magazine*, Jan., 2013.

[9] C. Ciochina, "A review of OFDMA and single-carrier FDMA", *2010 European Wireless Conference (EW)*, Page(s): 706-710, 2010.

[10] W.J. Van Houtum, "Single carrier digital terrestrial television broadcasting", *IEEE Transactions on Broadcasting*, Vol. 43, Issue: 4, Page(s): 403-411, 1997.

[11] X. Wang, Y. Wu, G. Gagnon, B. Tian, K. Yi, J.Y. Chouinard, "A Hybrid Domain Block Equalizer for Single-Carrier Modulated Systems", *IEEE Transactions on Broadcasting*, Vol. 54, Issue: 1, 2008.

[12] A. Pitarokoilis, S.K. Mohammed, E.G. Larsson, "On the Optimality of Single-Carrier Transmission in Large-Scale Antenna Systems", *IEEE Wireless Communications Letters*, Vol. 1, Issue: 4, 2012.

[13] S. Huang; J. Wang; J. Song, "A Receiver Diversity Scheme for Single-Carrier System With Unique Word", *IEEE Transactions on Broadcasting*, Vol. 58, Issue: 2, 2012.

[14] C. Lim, B. Lee, "Development of ATSC-MH receiver for mobile digital TV services", *IEEE Transactions on Consumer Electronics*, Vol.56, Issue: 3, 2010.

[15] W. Fischer, *Digital Video and Audio Broadcasting Technology*, Springer Berlin Heidelberg, 2010.

[16] Advanced Television Systems Committee, "Advanced Television Systems Committee Invites Proposals for Next-Generation TV Broadcasting Technologies". 2013-03-26. Retrieved 2013-04-15

[17] M. Sakurai, "Digital Television Receiver for ISDB", *Proceedings of the IEEE*, Vol. 94, Issue: 1, Page(s): 323-326, 2006.

[18] ETSI, "Digital Video Broadcasting (DVB); Framing structure, channel coding and modulation for digital terrestrial television", ETSI Standard: EN 300 744 V1.5.1.

[19] Y.Wu, "Performance comparison of ATSC 8-VSB and DVB-T COFDM transmission systems for digital television terrestrial broadcasting", *IEEE Transactions on Consumer Electronics*, 1999.

[20] S. Nakahara, S. Moriyama, T. Kuroda, M. Sasaki, S. Yamazaki, and O. Yamada, "Efficient Use of Frequencies In Terrestrial ISDB System", *IEEE Transaction On Broadcasting*, Vol. 42, No. 3, Page(s): 173-178, 1996.

[21] S. Moriyama, M. Takada, S. Nakahara, H. Miyazawa, "Progress Report of ISDB-T System", *Broadcast Asia*, 2000.

[22] J. Bingham, "Multicarrier modulation for data transmission: an idea whose time has come", *IEEE Communication Magazine*, Vol. 28, No. 5, Page(s): 5-14, 1990.

[23] M. Nakhai, "Multicarrier transmission", *IEEE Transactions on Signal Processing*, Vol. 2, Issue: 1, Page(s): 1-14, 2008.

[24] H. Li, B. Liu, and H. Liu, "Transmission schemes for multicarrier broadcast and unicast hybrid system", *IEEE Transactions on Wireless Communications*, Vol. 7, Issue: 11, Part 1, Page(s): 4321-4330, 2008.

[25] A. Erdozain, P. Crespo, B. Beferull-Lozano, "Multiple Description Analog Joint Source-Channel Coding to Exploit the Diversity in Parallel Channels", *IEEE Transactions on Signal Processing*, Vol. 60, Issue: 11, 2012.

[26] D. Tse, P. Viswanath, *Fundamentals of Wireless Communication*. Cambridge University Press, 2005.

[27] X. Shao, "A robust cross coding scheme for OFDM systems", *2010 International Symposium on Information Theory and its Applications (ISITA)*, Page(s): 282-287, Oct., 2010.

[28] DVB, *Upper Layer Forward Error Correction in DVB*, DVB Document A148, Mar., 2010.

[29] S. Papaharalabos, D. Benmayor, P. Mathiopoulos, P. Fan, "Performance Comparisons and Improvements of Channel Coding Techniques for Digital Satellite Broadcasting to Mobile Users", *IEEE Transactions on Broadcasting*, Vol. 57, Issue: 1, 2011.

[30] S. Liu, H. Li, B. Braaten, "Network Coverage in Multicarrier Broadcast System", *2010 IEEE Global Telecommunications Conference (GLOBECOM 2010)*, Page(s): 1- 5, Dec., 2010.

[31] D. Plets, W. Joseph, L. Verloock, L. Martens, P. Angueira, J. Arenas, "SFN gain in broadcast networks", *2011 IEEE International Symposium on Broadband Multimedia Systems and Broadcasting (BMSB)*, Page(s): 1-6, 2011.

[32] M. Tormos, C. Tanougast, A. Dandache, P. Bretillon, P. Kasser, "Experimental performance of mobile DVB-T2 in SFN and distributed MISO network", *19th International Conference on Telecommunications (ICT)*, 2012.

[33] O. Simone, O. Kramer, G. Poor, and H. Shamai, "Cellular systems with multi-cell processing and conferencing links between mobile stations", *IEEE Information Theory and Applications Workshop*, Page(s): 361-365, 2008.

[34] D.Gesbert, S. Hanly, H. Huang, S. Shamai Shitz, O. Simeone, W. Yu, "Multi-Cell MIMO Cooperative Networks: A New Look at Interference", *IEEE Journal on Selected Areas in Communications*, Vol. 28, Issue: 9, 2010.

[35] H. Li, S. Khan, and H. Liu, "Broadcast network coverage with multi-cell cooperation", *International Journal of Digital Multimedia Broadcasting*, Vol. 2010.

[36] W. Feng, Y. Li, S. Zhou, J. Wang, "Downlink Power Allocation for Distributed Antenna Systems in a Multi-Cell Environment", *5th International Conference on Wireless Communications, Networking and Mobile Computing*, 2009.

[37] C. Hu, L. Yuen, C. Zhang, Y. Zhang; Z. Rapajic, "Intrinsic measure of diversity gains in generalized distributed antenna systems with cooperative users", *IET Communications*, Vol. 3, Issue: 2, Page(s): 209-222, 2009.

[38] H. Dahrouj, Y. Wei, "Coordinated beamforming for the multicell multi-antenna wireless system", *IEEE Transactions on Wireless Communications*, Vol. 1, Issue: 2, Page(s): 1748-1759, 2010.

[39] J. Zhang, R. Zhang, G. Li, L.Hanzo, "Remote Coalition Network Elements for Base Station Cooperation Aided Multicell Processing", *IEEE Transactions on Vehicular Technology*, Vol. 61, Issue: 3, 2012.

[40] R. Zhang, S. Cui, "Cooperative interference management in multi-cell downlink beamforming", *IEEE Wireless Communications and Networking Conference (WCNC)*, Page(s): 1-5, 2010.

[41] H. Moon , "Waterfilling Power Allocation at High SNR Regimes", *IEEE Transactions on Communications*, Vol. 59, Issue: 3, 2011.

[42] Y. Ma ; D. Kim, " Rate-maximization scheduling schemes for uplink OFDMA", *IEEE Transactions on Wireless Communications*, Vol. 8, Issue: 6, 2009.

[43] A. Tulino, G. Caire, S. Shamai, S. Verdu, "Capacity of Channels With Frequency-Selective and Time-Selective Fading", *IEEE Transactions on Information Theory*, Vol. 56, Issue: 3, 2010.

[44] P. He, L. Zhao, S. Zhou, Z. Niu, "Recursive Waterfilling for Wireless Links With Energy Harvesting Transmitters", *IEEE Transactions on Vehicular Technology*, Vol. 63, Issue: 3, 2014.

[45] Y. Pan, A. Nix, M. Beach, "Distributed Resource Allocation for OFDMA-Based Relay Networks", *IEEE Transactions on Vehicular Technology*, Vol. 60, Issue: 3, 2011.

[46] C. Xiao, Y. Zheng, "On the Mutual Information and Power Allocation for Vector Gaussian Channels with Finite Discrete Inputs", *2008 IEEE GLOBECOM*, Page(s): 1-5, 2008.

[47] A. Goldsmith, *Wireless Communications*, New York: Cambridge University Press, 2005.

[48] DVB, *DVB-NGH, Next Generation Handheld*, `http://www.dvb.org/technology/dvb-ngh/index.xml`.

[49] Algolith White Paper, *Traditional Broadcasting in a World with New Options*, 2008.

[50] V. Garcia, N. Lebedev, J. Gorce, "Capacity Outage Probability for Multi-Cell Processing Under Rayleigh Fading", *IEEE Communications Letters*, Vol. 15, Issue: 8, 2011.

[51] W. Ao, K. Chen, "Broadcast Transmission Capacity of Heterogeneous Wireless Ad Hoc Networks with Secrecy Outage Constraints", *2011 Global Telecommunications Conference (GLOBECOM 2011)*, Page(s): 1-5, 2011.

[52] X. Kang, Y. Liang, H. Garg, "Fading Cognitive Multiple Access Channels: Outage Capacity Regions and Optimal Power Allocation", *IEEE Transactions on Wireless Communications*, Vol.9, Issue: 7, 2010.

[53] E. Teletar, "Capacity of multi-antenna Gaussian channels", *AT&T Bell Labs Internal Tech. Memo.*, 1995.

[54] Burger, R. Lacovoni, G. Reader, F. Xiaodong, Y. Hui, "A survey of digital TV standards China",*CHINACOM '07,* Page(s): 687, Aug., 2007.

[55] R. Yamasaki, M. Takada, H. Hamazumi, K. Shibuya, "High-speed mobile reception of HDTV in ISDB-T with directional diversity reception method using adaptive array antenna", *IEEE Radio and Wireless Symposium,* 2009.

[56] J. Laneman, E. Martinian, G. Wornell, Source channel diversity for parallel channels", *IEEE Transaction on Information Theory,* Vol. 51, No. 10, Page(s): 3518-3539, 2005.

[57] F. Hartung, U. Horn, "Delivery of broadcast services in 3G networks", *IEEE Transaction on Broadcasting,* Vol. 53, No. 1, Page(s): 188-199, 2007.

[58] U. Reimers, "DVB-The family of international standards for digital video broadcasting",*Proceedings of the IEEE*, Page(s): 173-182, 2006.

[59] M. Chari, F. Ling, A. Mantravadi, R. Krishnamoorthi, R. Vijayan, G. Walker, and R. Chandhok, "FLO Physical Layer: An Overview", *IEEE Transactions on Broadcasting,* Vol.53, Page(s): 145-160, 2007.

[60] O. Somarriba and T. Giles, "Transmission control for spatial TDMA in wireless radio networks", *IEEE International Workshop on Mobile and Wireless Communications Network,* Page(s): 394-398, 2002.

[61] S. Yoon and D. Kim, "System level performance of broadcast/unicast service overlay using superposition coding", *IEEE International Symposium on Personal, Indoor and Mobile Radio Communications,* Page(s): 1-5, 2007.

[62] M. Costa, "Writing on dirty paper", *IEEE Trans. Information Theory,* Vol. 29, No. 3, Page(s): 439-441, May, 1983.

[63] M. Sharif and B. Hassibi,"A comparison of time-sharing, DPC, and beam forming for MIMO broadcast channels with many users", *IEEE Transactions on Communications,* Vol. 55, No. 1, Page(s): 11-15, 2007.

[64] S. Gaur, J. Acharya, and L. Gao, "Enhancing ZF-DPC performance with receiver processing", *IEEE Transactions on Wireless Communications,* Vol. 10, No. 12, Page(s): 4052-4056, 2011.

[65] B. Liu, H. Li, H. Liu and S. Roy, "DPC-based hierarchical broadcasting: design and implementation", *IEEE Transactions on Vehicular Technology,* Vol. 57, No. 6, Page(s): 3895-3900, November, 2008.

[66] H. Li, B. Liu, and H. Liu, "Transmission Schemes for Multicarrier Broadcast and Unicast Hybrid Systems", *IEEE Transactions on Wireless Communications,* Vol. 7, pp. 1169-1173, 2008.

[67] S. Liu, H. Li, G. Ru, W. Lin, L. Liu and Y. Yi; "Capacity of Multicarrier Multilayer Broadcast and Unicast Hybrid Cellular System with Independent Channel Coding over Subcarriers", 2011 IEEE Vehicular Technology Conference (VTC Fall), Page(s): 1-3, 2011.

[68] D. Tse, P. Viswanath, Fundamentals of Wireless Communication, *Cambridge University Press*, 2005.

[69] H. Weingarten, Y. Steinberg, S. Shamai, "The capacity region of the Gaussian Multiple-Input Multiple-Output broadcast channel", *IEEE Transactions on Information Theory,* Vol. 52, Issue: 9, Page(s): 3936-3964, 2006.

[70] Edward Neuman, "Inequalities and Bounds for the Incomplete Gamma Function", *Results in Mathematics,* Vol. 63, Issue: 3-4, Page(s): 1209-1214, Jun, 2013.

[71] M. Rafiei, S. Eftekhari, "A practical smart metering using combination of power line communication (PLC) and WiFi protocols", *17th Conference on Electrical Power Distribution Networks* (EPDC), Page(s): 1-5, 2012.

[72] T. Banwell, S. Galli, "A novel approach to the modeling of the indoor power line channel part I: circuit analysis and companion model", *IEEE Transactions on Power Delivery*, Vol. 20, Issue: 2, Part: 1, Page(s): 655-663, 2005.

[73] M. Zimmermann and K. Dostert, "An analysis of the broadband noise scenario in powerline networks", *Proc. Int. Symp. Powerline Communications and its Applications*, Page(s): 131-138, Apr., 2000.

[74] G. Matthias, M. Rapp, and K. Dostert, "Power line channel characteristics and their effect on communication system design", *IEEE Communication Magazine*, Vol. 42, Page(s): 78-86, Apr., 2004.

[75] F. J. Canet, L. Diez, J. A. Cortes, and J. T. Entrambasaguas, "Broadband modeling of indoor power-line channels", *IEEE Trans. Consumer Electronics*, Vol. 48, No. 1, Page(s): 175-183, Feb., 2002.

[76] T. Esmailian, R. F. Kschischang, and P. G. Gulak, "In-building power lines as high-speed communication channels: Channel characterization and a test channel ensemble", *International Communication System*, Page(s): 381-400, 2003.

[77] J. Abad, A. Badenes, J. Blasco, J. Carreras, V. Dominguez, C. Gomez, S. Iranzo, J. C. Riveiro, D. Ruiz, and L. M. Torres, "Extending the power line LAN up to

the neighborhood transformer",*IEEE Communication Magazine*, Vol. 41, No. 4, Page(s): 64-70, Apr., 2003.

[78] D. Liu, E. Flint, B. Gaucher, and Y. Kwark, "Wideband AC powerline characterization", *IEEE Transaction Consumer Electronics*, Vol. 45, No. 4, Page(s): 1087-1097, Nov., 1999.

[79] P. Amirshahi and M. Kavehrad, "Transmission channel model and capacity of overhead multi-conductor medium-voltage power-lines for broadband communications", *Proc. CCNC*, Las Vegas, NV, Page(s): 354-358, Jan., 2005.

[80] Anatory, M. M. Kissaka, and N.H. Mvungi, "Broadband Power-Line Communications: The Channel Capacity Analysis", *IEEE Trans. on Power Delivery*, Vol. 23, No. 1, Jan., 2008.

[81] H.Meng, S.Chen, Y.L.Guan, C.L.Law, P.L.So, E.Guanawan and T.T.Lie, "Modeling of transfer characteristics for the broadband power line communication channel", *IEEE Trans. Power Delivery*, Vol.19, No. 3, Page(s): 1057-1064, Jul., 2004.

[82] A.G.Lazaropoulos and P.G.Cottis, "Transmission characteristics of overhead medium voltage power line communication channels", *IEEE Trans. Power Del.*, Vol.24, No.3, Page(s): 1164-1173, Jul.,2009.

[83] E. Liu, Y. Gao, G. Samdani, O. Mukhtar, and T. Korhonen, "Broadband power line channel and capacity analysis", *Proc. IEEE-ISPLC*, Vancouver, BC, Canada, Page(s): 7-11, Mar., 2005.

[84] J. Anatory, M. M. Kissaka, and N.H. Mvungi, "Channel model for broadband power-line communications", *IEEE Trans. Power Del.*, Vol. 22, No. 1, Page(s): 131-145, Jan., 2007.

[85] P. Amirshahi and M. Kavehrad, "High-frequency characteristics of overhead multiconductor power lines for broadband communications", *IEEE Journal of Selected Areas of Communication*, Vol. 24, No. 7, Page(s): 1292-1303, Jul., 2006.

[86] J. Marti, "Accurate Modeling of Frequency-Dependent Transmission Lines in Electromagnetic Transient Simulations", *IEEE Power Engineering Review*, Vol. 2, Issue: 1, Page(s): 29-30, 1982.

[87] A. Semlyen, "Contributions to the Theory of Calculation of Electromagnetic Transients on Transmission Lines with Frequency Dependent Parameters", *IEEE Transactions on Power Apparatus and Systems*, Vol. PAS-100, Issue: 2, Page(s): 848 - 856, Feb., 1981.

[88] A. Semlyen, A. Roth, "Calculation of Exponential Step Responses - Accurately for Three Base Frequencies", *IEEE Transactions on Power Apparatus and Systems*, Vol. 96, No. 2, Page(s): 667-672, Mar., 1977.

[89] S. Fan; Y. Li; X. Li; L.Bi ,"A Method for the Calculation of Frequency-Dependent Transmission Line Transformation Matrices", *IEEE Transactions on Power Systems*, Vol. 24, Issue: 2, Page(s): 552-560, May, 2009.

[90] Y. Chen; V. Dinavahi, "Digital hardware emulation of universal machine and universal line models for real-time electromagnetic transient simulation", *2012 IEEE Power and Energy Society General Meeting*, Page(s): 1-10, 2012.

[91] Y. Liao; M. Kezunovic, "Online Optimal Transmission Line Parameter Estimation for Relaying Applications", *IEEE Transactions on Power Delivery*, Vol. 24, Issue: 1, Page(s): 96-102, Jan., 2009.

[92] A. Semlyen, A. Ramirez, "Direct Frequency Domain Computation of Transmission Line Transients Due to Switching Operations", *IEEE Transactions on Power Delivery*, Vol. 23, Issue. 4, Page(s): 2255-2261, Oct., 2008.

[93] T.T. Nguyen, "Phase-domain transmission circuit model for electromagnetic transient analysis-representation of characteristic impedance matrix by a passive network", *IEEE Power and Energy Society General Meeting*, Jul, 2010.

APPENDIX. POWER-LINE CHANNEL IN TRANSIENT MODEL

In recent years, power transmission lines have been used to provide broadband data access using indoor, low-voltage, and medium-voltage channel topologies. This technology involves interconnecting one municipality with others to provide alternative information and communications technology (ICT) in developed and developing countries. On the other hand, power line communication (PLC) can also be used for narrowband communications in power system operations, such as automatic meter reading, circuit break status monitoring, etc. In addition, by combining with wireless networks such as wireless local-area network (WLAN) and WI-FI [71], it is possible to apply the fourth-generation mobile communication system over PLC. [1]

As a well-established major infrastructure, the power-line was originally designed to transmit the electrical power. However, from data communication perspective, PLC experiences severe signal reflection and divergence (i.e., undesired multipath effect) due to impedance mismatch between the existing branch lines and the receiving terminal's loads on the power line. Therefore, even though the power line could serve as a wired communication channel, its data transfer characteristics are very similar to (or even worse than) those of a typical wireless channel. Furthermore, since power network topology and load vary all the time, the parameters of the multipath channels are also time varying with a large dynamic.

To achieve efficient PLC, a power line channel's performance has to be evaluated with higher accuracy so suitable PLC equipment can be designed accordingly (e.g. routers, multiplexer). For this reason, many researchers attempted to develop appropriate channel models for power lines. The earliest model was established for the use of indoor applications by Banwell and Galli [72]. For low/voltage applications, Zimmermann and Dostert have proposed a design of the communication system using

[1] This part of work has been published on IEEE Transaction on Power Delivery

the power line [73],[74]. According to Shannon's formula, in order to evaluate the capacity of the power line communication system, an appropriate model for the power line channel is needed. Generally, there are two main categories of power line channel models: time-domain models and frequency-domain models [75]-[79]. However, the above models did not present analytical methods for calculating channel transfer functions (CTF) [80]. Recently, channel models based on transmission and reflection factors in conjunction with the propagation constants were proposed in [81]-[85] for a PLC network system with two-conductor transmission-line (TL) which is modeled as a lumped-circuit π model. These models provide some theoretical insights on PLC channel characteristics, it cannot accurately reflect the variation of the CTF compared with the actual measurements. This is because the model neglected the generalized transmission-line theory and considered only the transmission and reflection factors at nodes or junctions with an appropriate propagation factor. In order to obtain the accurate formulation of the CTF, a generalized TL approach is adapted to determine the channel responses. However, the models utilized in these papers are still based on the lumped-circuit π model of the transmission line, which is not able to describe the change of the channel transfer characteristic when transients occur in the network.

In this part, we derive the CTF under the power line transient model. Specifically, we adopt the J. Marti Model [17] for the analytical derivation. The channel frequency responses are derived for different TL lengths and terminal loads. Comparing with previous work, the transient model we utilized can describe more accurately the variation of the channel frequency responses, especially when transients occur on the TL. Simulation results show that higher accuracy is achieved comparing with the results under the traditional lumped-circuit π model.

In order to study the channel frequency response, we focus on the calculation in frequency domain and all variables are represented as a function of frequency. The

frequency-dependent TL models are based on J. Marti's representation where the line characteristic impedance and propagation function are expressed as a sum of exponential terms in time domain [86].

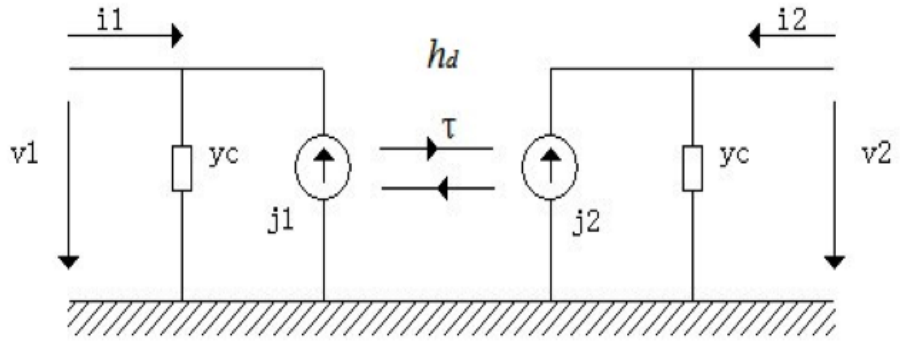

Figure A.1. The equivalent circuit of Marti's model

J. Marti Model is relatively computationally inexpensive and accurate in a wide range of frequencies. Figure A-1 illustrates the Marti's transient model of a typical TL, where the overall channel $h(t)$ of the TL is modeled as an equivalent characteristic admittance y_c at both ends plus a lossless channel h_d between j_1 and j_2 with delay τ. Specifically, the J. Marti Model approximates the frequency dependent parameters of lines and cables into rational functions, and then these functions are replaced by an equivalent circuit. This circuit can reproduce all the characteristics of lines and cables. The mathematical representations are given as follows:

$$j_1(t) = h_d(t) * [y_c(t) * v_2(t-\tau) + i_2(t-\tau)] \tag{A.1}$$

$$j_2(t) = h_d(t) * [y_c(t) * v_1(t-\tau) + i_1(t-\tau)] \tag{A.2}$$

where "*" denotes the convolution operation and v_1, i_1, v_2, i_2 are the voltage and current on the transmitting and receiving ends. The evaluation of the convolution

integrals by efficient recursive schemes requires y_c to be as a sum of exponential :

$$y_c(t) = Y_\infty + \sum_{k=1}^{m} Y_k e^{-\lambda_k t} \tag{A.3}$$

where $\{\lambda_k\}$ are delay factors defined in [87] and they are mainly induced by the length of TL; $\{Y_k\}$ are coefficients used in the rational fitting algorithm [87]. Note that accurate representation of $H(\omega)$ substantially depends on $y_c(t)$.

Denote I_m as the transmitted signals, by using the TL theory, the transfer function relating voltage at any point on the line can be calculated as:

$$\frac{dV(z,\omega)}{dz} = -Z(\omega)I(z,\omega) \tag{A.4}$$

$$\frac{dI(z,\omega)}{dz} = -Y(\omega)V(z,\omega) \tag{A.5}$$

where $V(z,\omega)$, $I(z,\omega)$ are line voltage and current at a point z km away from the load, $Z(\omega) = R(\omega) + j\omega L(\omega)$ is series impedance per unit length where R is the resistance and L is the inductance of the TL. $Y(\omega) = G + j\omega C$ is the shunt admittance per unit length where G is the reactance and C the capacitance of the TL. Solving the above equations simultaneously, we can obtain the values of voltage and current at any point of TL for any frequency:

$$V_2(\omega) = cosh[\gamma(\omega)l]V_1(\omega) - Z_c(\omega)sinh[\gamma(\omega)l]I_1(\omega) \tag{A.6}$$

where $V_2(\omega)$ is the line voltage at the point l km away from the load end and $V_1(\omega)$, $I_1(\omega)$ are the line voltage and current at the load. $Z_c(\omega)$ is the characteristic impedance of the line and $\gamma(\omega)$ is the propagation factor, which are given by:

$$Z_c(\omega) = \sqrt{\frac{Z(\omega)}{Y(\omega)}} \tag{A.7}$$

$$\gamma(\omega) = \sqrt{Z(\omega)Y(\omega)} \tag{A.8}$$

For Equations (A.1) and (A.2), we use Fourier transform to get their frequency domain representation as: $J_1(\omega) = H_d(\omega)[Y_c(\omega)V_1(\omega)+I_1(\omega)]e^{-j\omega\tau}$, $J_2(\omega) = H_d(\omega)[Y_c(\omega)V_2(\omega)+I_2(\omega)]e^{-j\omega\tau}$.

Since h_d is modeled as a lossless channel with delay τ, its transfer function is $H_d(\omega) = e^{-j\omega\tau}$ so that $H_d(\omega)e^{-j\omega\tau}$ [88]-[91]. Therefore, the frequency domain representation can be re-written as:

$$-I_1(\omega) = Y_c(\omega)V_1(\omega) - J_1(\omega)e^{2j\omega\tau} \tag{A.9}$$

$$-I_2(\omega) = Y_c(\omega)V_2(\omega) - J_2(\omega)e^{2j\omega\tau} \tag{A.10}$$

Thus, the transfer function between the source and the end point of a power line is given as:

$$H(\omega) = \frac{I(\omega)}{I_s(\omega)}\frac{Z_c(\omega) + Z_s(\omega)}{Z_c(\omega)} \tag{A.11}$$

where $I_s(\omega)$ and $I(\omega)$ are the source current and the current on the line, $Z_s(\omega)$ is the source impedance and $Z_c(\omega)$ is the impedance of the entire TL as defined in Equation (A.7).

Assume the received current is $-I_2$ (the direction of I_1 is positive) in Equation (A.11), we can take Equation (A.9) into (A.11) and have the following results:

$$H(\omega) = \frac{Z_c(\omega) + Z_s(\omega)}{Z_c(\omega)}[Y_c(\omega)V_2(\omega) - J_2(\omega)e^{2j\omega\tau}] \tag{A.12}$$

$$V_2(\omega) = cosh[\gamma(\omega)l]V_s(\omega) - Z_c(\omega)sinh[\gamma(\omega)l]I_s(\omega) \tag{A.13}$$

$$J_2(\omega) = [Y_c(\omega)V_s(\omega) + I_s(\omega)]e^{2j\omega\tau} \tag{A.14}$$

$$Y_c(\omega) = F\{Y_\infty + \sum_{k=1}^{m} Y_k e^{-\lambda_k t}\} \tag{A.15}$$

where F denotes the Fourier transform from time domain to frequency domain. Y_∞ is the impedance of the source.

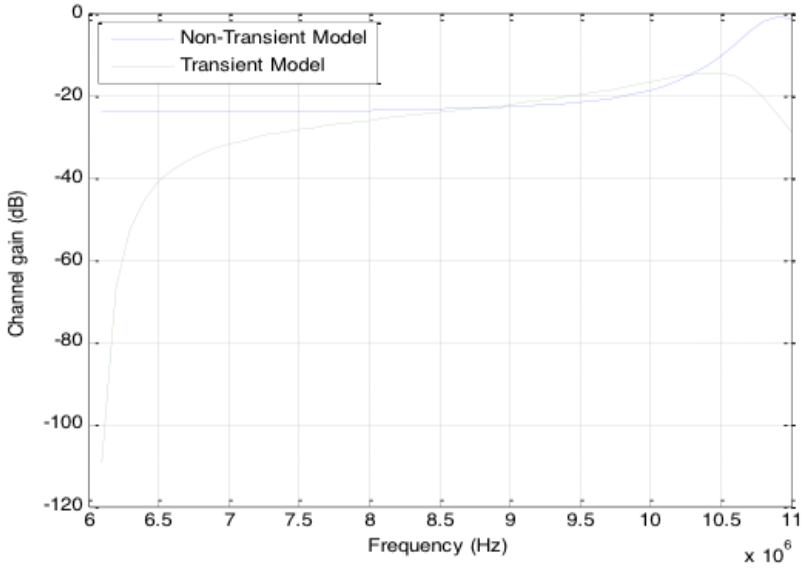

Figure A.2. Comparison of channel gain change

Based on Equations (A.12) - (A.15), we can simulate the CTF gain $H(\omega)$ under the transient model. In Figures A.2 and A.3, we compare the channel gain characteristics under the Marti's transient model and the model in [84]. For fair comparison, we set the same parameters of the TL as in [84]. Without any branch or nodes on the TL, Figures A.2 and A.3 show that between 6MHz and 8MHz and beyond 10.5MHz, the transient model provides more details of the phase variation than the non-transient model. For the rest of the frequency domain, the two models have similar performance.

For more complicated and practical TL with additional nodes and branches in the middle, Figure A.4 shows that the transient model not only provides more details of the phase variation.

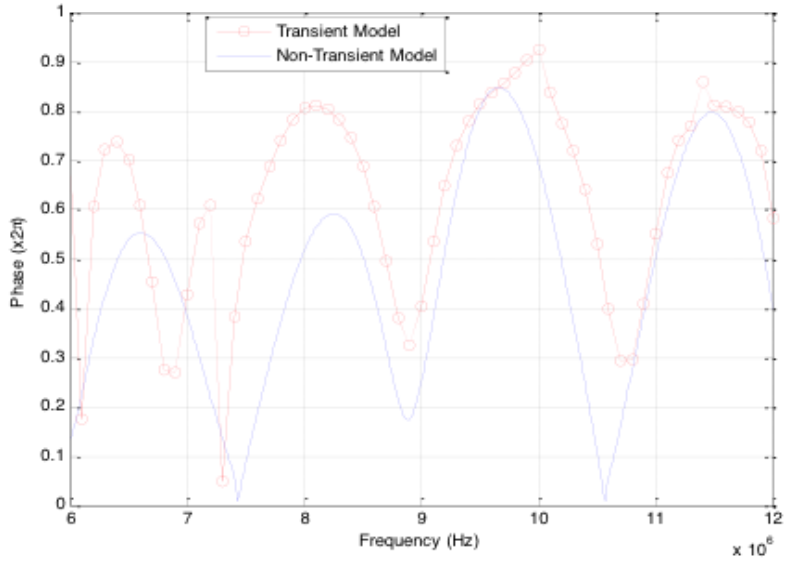

Figure A.3. Comparison of phase change

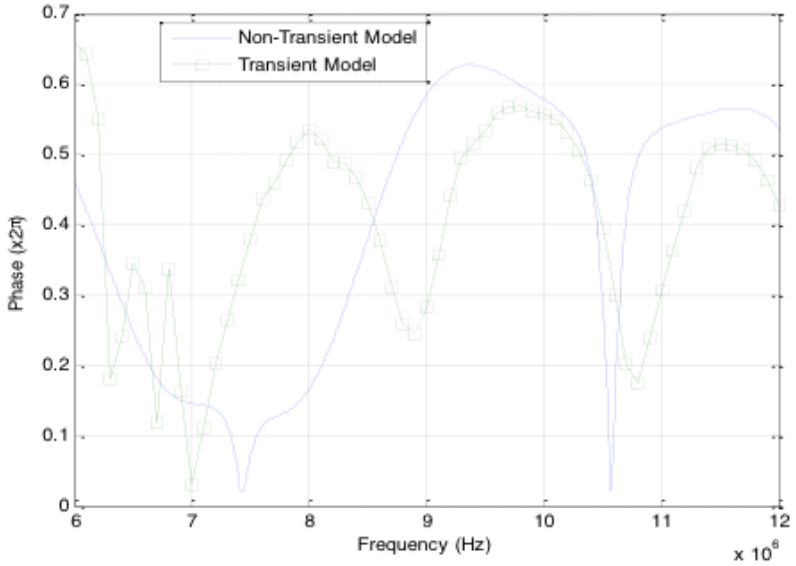

Figure A.4. Comparison of phase transients for TL

The phase is also quite different from that of the non-transient model for the entire frequency domain. This is because with more nodes and branches, the transients of the signal become more significant. The detailed discussion on the impact of the nodes and branches will be covered latter.

Besides showing more details on the variation of the channel, another advantage of the transient model is that it can reflect the variation of the channel characteristics when transient events occur in the power system, e.g. the switch is turned on/off, one or more lines touch the ground or two lines touch each other, which cannot be reflected by non-transient models.

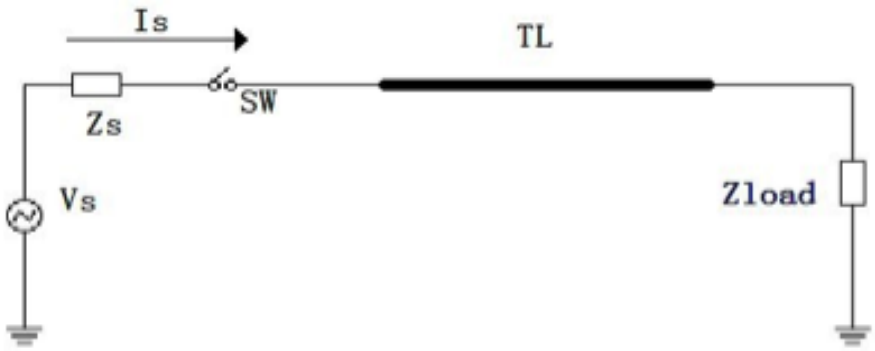

Figure A.5. Single-diagram for three-phase TL

In Figure A.5, a single-diagram for a three-phase TL is shown as an illustration. We first consider the transients caused by closing the switch. The voltage across the switch is:

$$Y_{sw}(\omega) = V_s(\omega) - ZI_s(\omega) \tag{A.16}$$

$$Z = Z_s + [Y_s - Y_m(Y_s + Y_l)^{-1}Y_m)]^{-1} \tag{A.17}$$

where $Y_s = Y_c coth(\gamma l)$,$Y_m = -Y_c csch(\gamma l)$. $Y_c = 1/Z_c$ is the characteristic admittance and Y_l is the load. The parameters γ and l indicated the propagation factor and TL length respectively. According to [92], the TL transients can be computed directly

on frequency domain as:

$$I_s(\omega) = YV_s(\omega) \tag{A.18}$$

$$Y_{ON} = \bar{U}_{ON}(U_{ON}^T Z \bar{U}_{ON})^{-1} U_{ON}^T \tag{A.19}$$

$$U = [U_{ON}, U_{OFF}]^T, W = N[\bar{U}_{ON}, \bar{U}_{OFF}] \tag{A.20}$$

where W and U are the matrices corresponding to fast Fourier Transform (FFT) and inverse fast Fourier Transform; $U_{ON}^T, U_{OFF}^T, \bar{U}_{ON}, \bar{U}_{OFF}$ are partitions of U and W according to the time segments when the switch is on or off; N is the total number of sampling point. By plugging (A.18) and (A.19) into (A.12)-(A.15), we have:

$$H(\omega) = \frac{Y_c + Y_s}{Y_s}[Y_{ON}^{-1} Y_c cosh(\gamma l) - sinh(\gamma l)(Y_{ON}^{-1} Y_c - 1)e^{2j\omega\tau}] \tag{A.21}$$

Similarly, for the case of switch off, we just need to change Y_{ON} in Equation (A.21) as Y_{OFF}, which is defined as follow:

$$Y_{OFF} = \bar{U}_{OFF}(U_{OFF}^T Z \bar{U}_{OFF})^{-1} U_{OFF}^T \tag{A.22}$$

Based on Equation (A.21), we can simulate the PLC transient response of switch on and off. Figure A.6 shows the transient behaviors of the channel gain by considering a source switch on and off. By comparing the two curves, we observe that the channel gain has relatively opposite performance under the two transient situations. However, for the case of opening a switch, the channel gain is higher than that of closing a switch in most part of the frequency domain.

Figure A.7 illustrates the variations of the transient channel gain at the moment when a 200 meter TL touches the ground at the middle of the line. We can see that the channel gain truncation frequencies are symmetric around 8MHz.

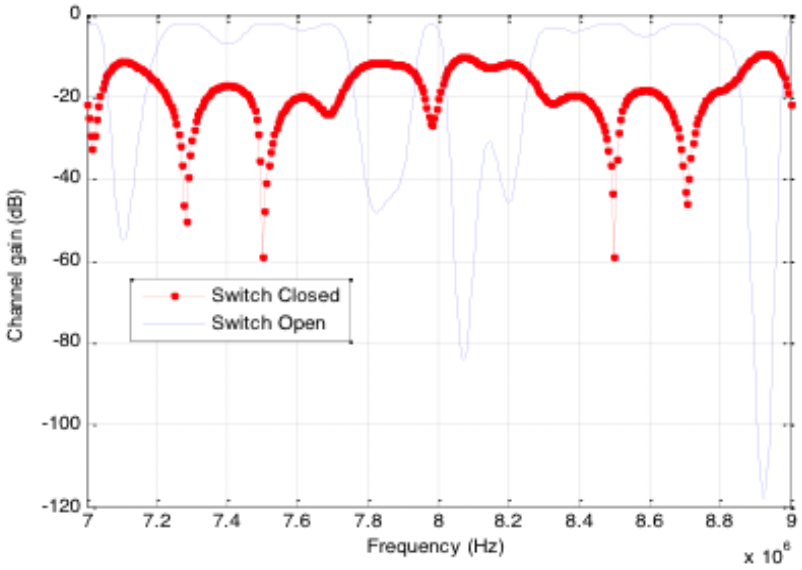

Figure A.6. Transient channel gain for switch on/off

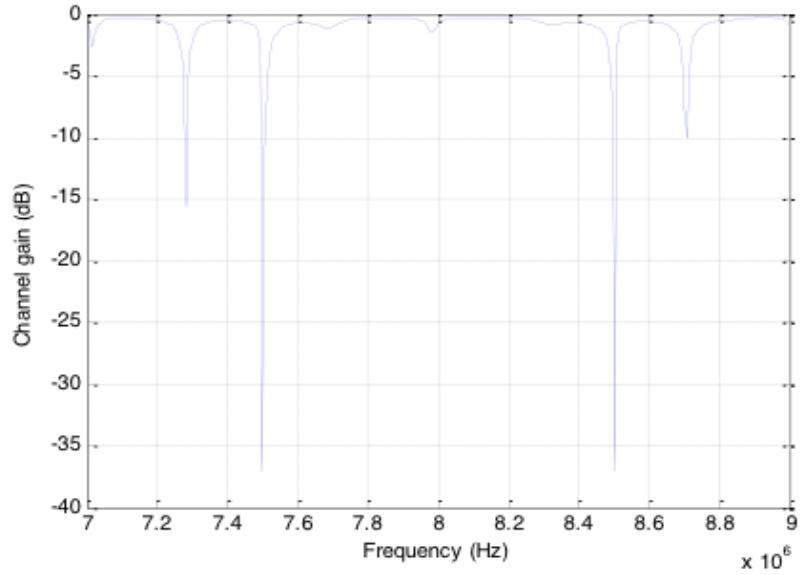

Figure A.7. Transient channel gain for TL (200m) touches ground

This can be explained by Equations (A.12) -(A.15): when the line touches the ground at the point k meters away from the source, Equation (A.13) becomes:

$$0 = cosh[\gamma(\omega)l]V_s(\omega) - Z_c(\omega)sinh[\gamma(\omega)l]I_s(\omega) \tag{A.23}$$

In Equation (A.23), the source voltage $V_s(\omega)$ and current $I_s(\omega)$ are known. In addition, since the line touches the ground, the load impedance becomes zero. Note that $Z_c(\omega)$ only consists of the impedance of the TL, which can be calculated by using the formula in [93] under transient analysis. Thus, we can solve Equation (A.23) to obtain the corresponding solutions of ω.

Using a similar approach, let us consider an extreme case in which a TL with a length of 1500 meters touches the ground at the location 10 meters away from the source. By using the above analysis and taking $k = 10$ in (A.23), we can obtain $\omega_1 = 3.283MHz$, $\omega_2 = 3.511MHz$, $\omega_3 = 4.47MHz$, $\omega_4 = 4.72MHz$. Taking those values of ω into Equation (A.11), we can calculate the corresponding channel gains at each frequency: -24.7dB, -4.8dB, -0.4dB and -0.02dB. Comparing the above values with the simulation results in Figure A.8, we can see that the analysis matches the simulation very well.

Next, let us consider the same TL with a length of 1500 meters touching the ground at a location close to the impedance end. By setting $k = 1450$, we assume the line touches the ground at the location 50 meters away from the impedance end. By solving Equation (A.23), we get $\omega_1 = 2.33MHz$, $\omega_2 = 2.61MHz$, $\omega_3 = 3.52MHz$, $\omega_4 = 3.74MHz$, which matches with the simulation result in Figure A.9.

A direct result caused by the variation of the channel gain is the degradation of the communication performance. In order to evaluate the performance of a communication system, bit error probability (BER) P_B under some specific signal-to-noise ratio (SNR) is often used.

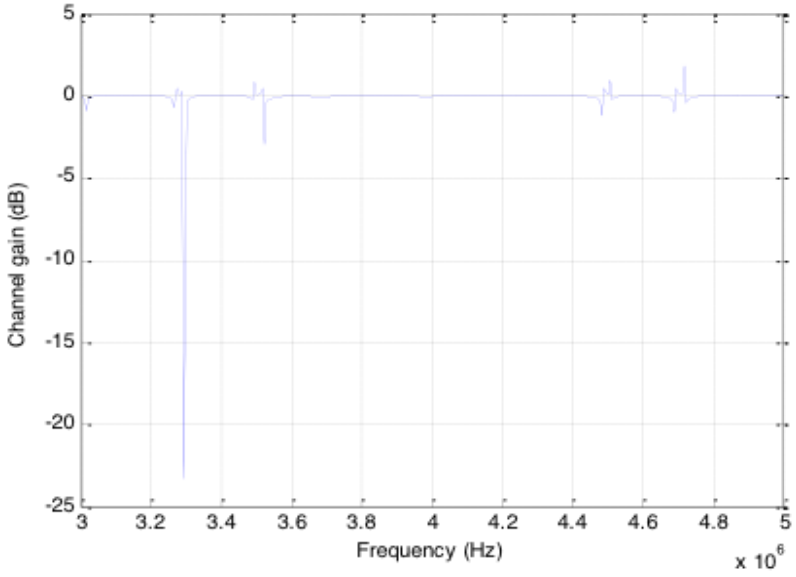

Figure A.8. Transient channel gain for TL (1500m) touches ground at source end

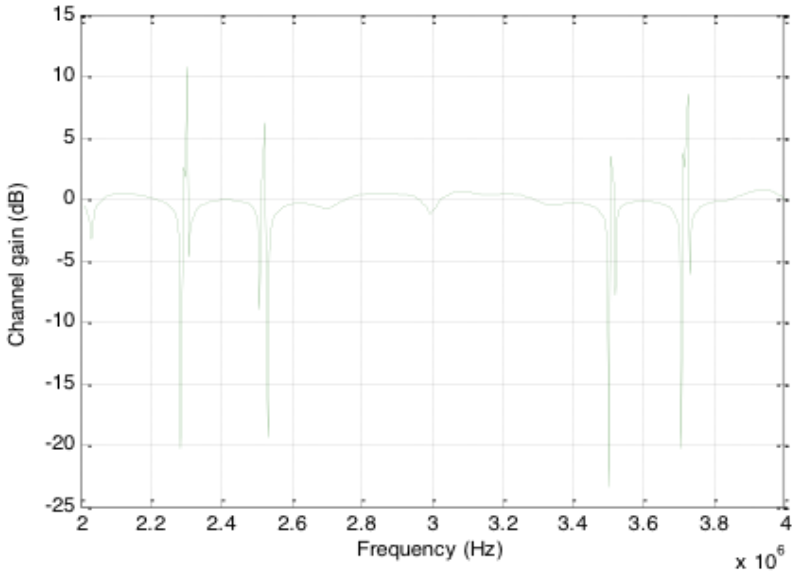

Figure A.9. Transient channel gain for TL (1500m) touches ground at load end

We assume that the noise in the channel follows Gaussian distribution of zero mean and variance N_0. Compared with the TL length, the branches's length on the TL is very small thus the delay profile of the channel is relatively small. On the other hand, due to the stability of the power network, we can assume the channel is unchanging during one symbol-duration. Hence, under this condition, we can assume the TL is a slow- and flat-fading channel.

In simulation, Binary Phase Shift Keying (BPSK) is chosen as the modulation scheme due to its easy implementation and low complexity. Under BPSK, the BER of a TL channel can be expressed as:

$$P_B = \frac{1}{4(E_B/N_0)\mathbf{E}(\alpha^2)} \tag{A.24}$$

where E_B is the energy of each transmitted bit and α^2 is a chi-square distributed random variable having the probability density function (PDF) as follow:

$$f(\alpha^2) = \frac{1}{\sigma^2} exp(-\frac{\alpha^2}{\sigma^2}) \tag{A.25}$$

The average path loss σ^2 is a function of carrier frequency and the TL length. The σ^2 can be calculated as:

$$\sigma^2 = (k_1\sqrt{f} + k_2 f)l \tag{A.26}$$

where f is the carrier-frequency and l is the TL length. Constant k_1 and k_2 can be found for a set of published attenuation figures for different TL types.

In Figure A.10 and Figure A.11, we compare the BER of a 200 meter TL under different transients. From both Figures, we can see that when transients occurred in the TL, the BER increases. This is because when transients generate different orders of harmonics as interferences.

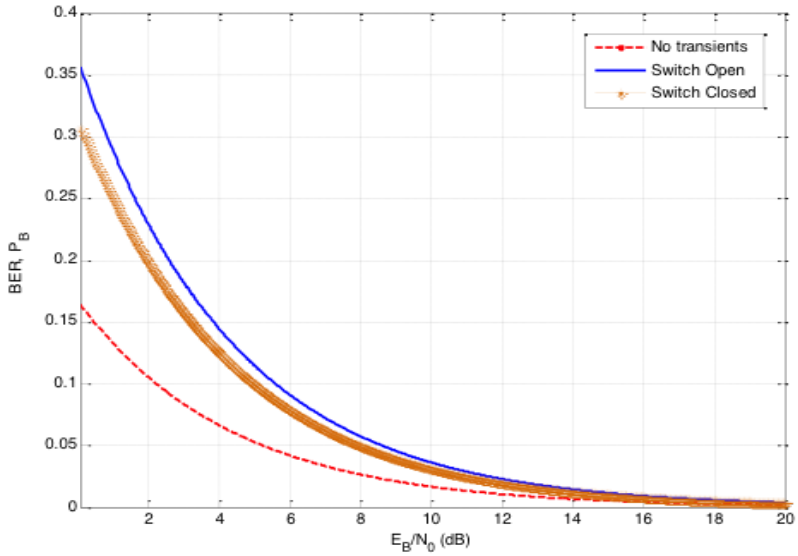

Figure A.10. Performance of BPSK over PLC ($f_c = 7.8MHz$)

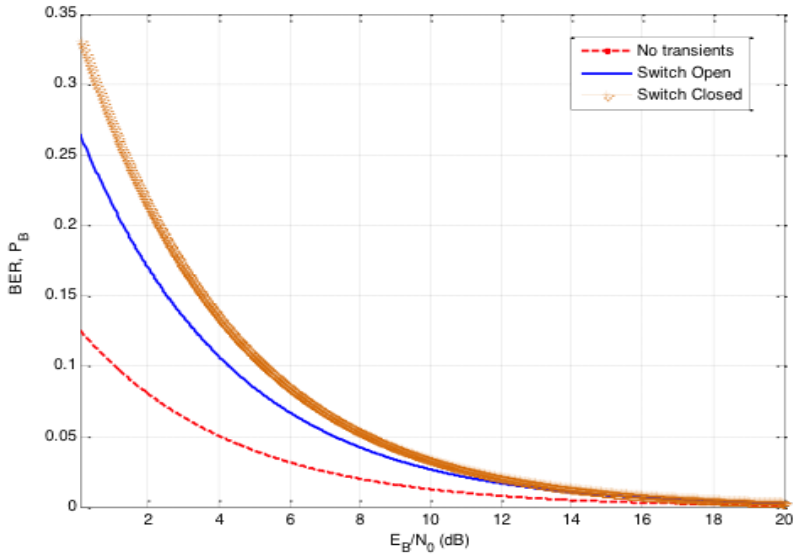

Figure A.11. Performance of BPSK over PLC ($f_c = 8.6MHz$)

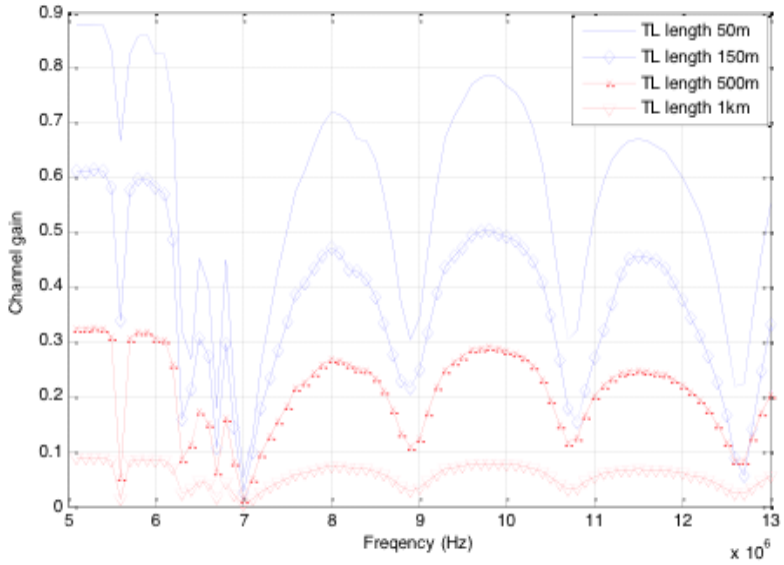

Figure A.12. Channel gain under different line lengths

In Figure A.10, we can see that opening a switch has larger BER than closing a switch. This is mainly because at $f_c = 7.8MHz$, the channel gain under the switch open case is larger, which coincides to the results in Figure 6. Similarly, the same conclusion can be drawn by comparing Figure 11 with Figure 6 at $f_c = 8.6MHz$.

From Equations (A.11) and (A.12), we can see that the main effect of the TL to the characteristic function comes from the term $V_2(\omega)$. Since $cosh[\gamma(\omega)l]$ decreases and $sinh[\gamma(\omega)l]$ increases with the length l, the channel gain $|H(\omega)|$ decreases with the TL length.

Figure A.12 shows the channel gain characteristics under different TL length. It clearly shows that the channel gain decreases with the TL length. This result coincides with our conclusion obtained from the analysis of Equations (A.11) and (A.12). Meanwhile, from signal transmission perspective, a longer line always leads to a larger signal fading (i.e., lower channel gain).

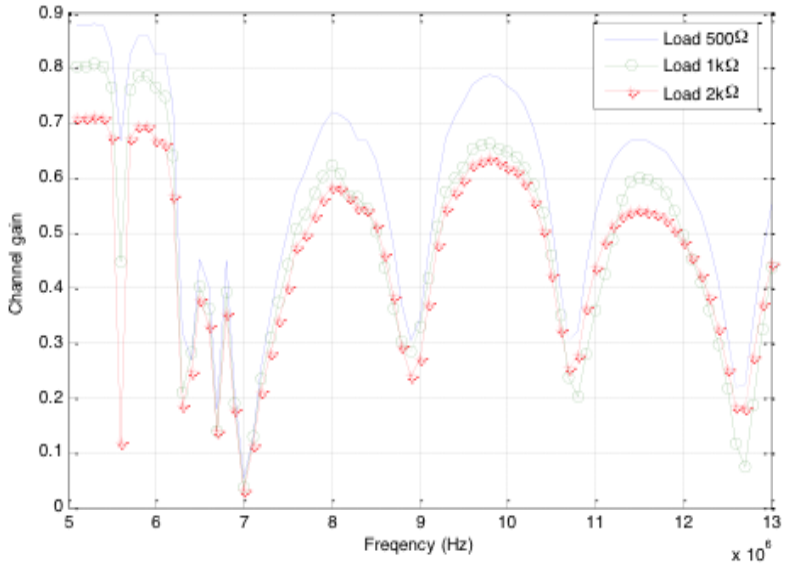

Figure A.13. Channel gain under different load impedance

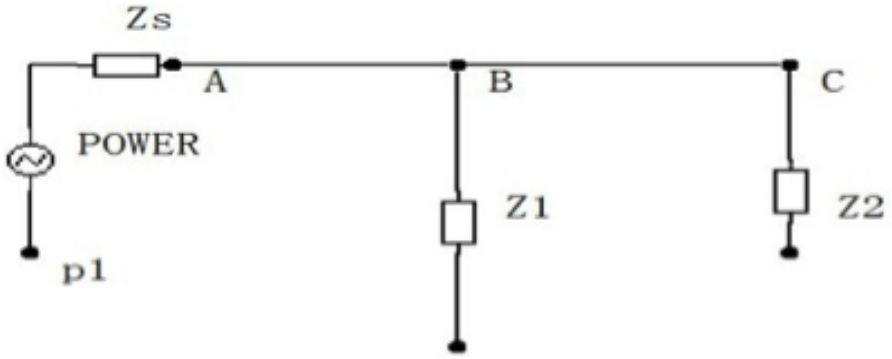

Figure A.14. TL with node and branch

Based on Equation (A.11), we have:

$$H(\omega) = \frac{1}{I_s(\omega)}[1 + \frac{Z_s(\omega)}{Z_c(\omega)}][Y_c(\omega)V_2(\omega) - J_2(\omega)e^{2j\omega\tau}] \tag{A.27}$$

Equation (A.27) implies that $|H(\omega)|$ decreases with $Z_c(\omega)$. Thus, the larger the load impedance is, the smaller $|H(\omega)|$ will be. Figure A.13 shows the simulation result of the channel gain under different load impedance, which is consistent to the above analysis.

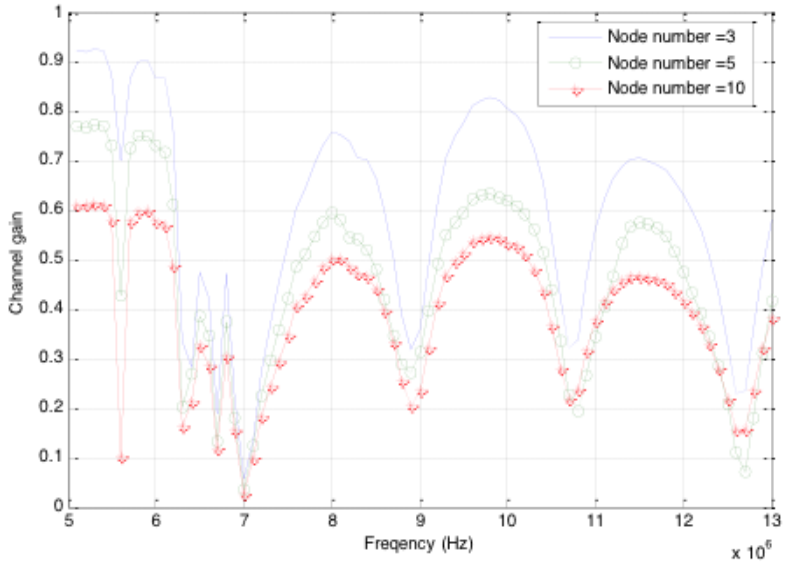

Figure A.15. Channel gains for different node numbers

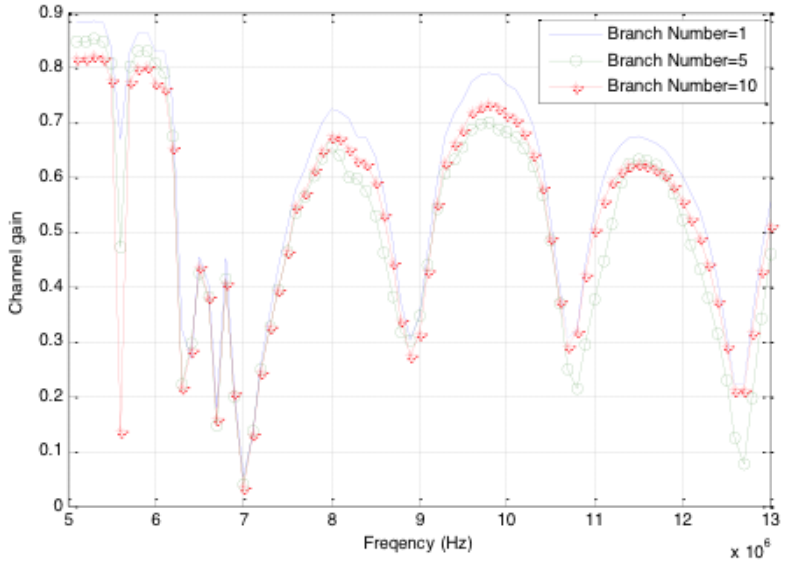

Figure A.16. Channel gains of different branch number

When TL length and load impedance are fixed, we study the effect of the number of branches on a specific node. Figure A.14 presents a typical TL with two nodes B and C. Each node is attached by a new branch Z_2 and Z_3 respectively. From Equation (A.11), the effect of the number of branches on channel gain $|H(\omega)|$ mainly comes from the term $J_2(\omega)$. The larger $J_2(\omega)$ is, the smaller $|H(\omega)|$ will be. According to Equation (A.16), $H_d(\omega)$ is mainly determined by the number of nodes n. A larger n yields a larger $J_2(\omega)$. Similar relationship exists between $J_2(\omega)$ and $Y_c(\omega)$. As a result, $|H(\omega)|$ decreases with the number of nodes and branches, . Simulation results in Figures A.15 and A.16 justify our above analysis.

Comparing our results from Figure A.13 to A.16 with those in [85], we can conclude that the TL parameters have a similar influence on the channel for both transient and non-transient models.

In this part, we discussed the channel gain characteristics of a power-line communication system under the J. Marti Model for transient analysis. The analytical formula of channel frequency response was derived based on the source-impedance relationship. We compared the variations of the CTFs between our model and other non-transient models. Results show that the transient model can accurately describe the variation of the channel frequency responses when transients occur on the transmission line,. Furthermore, we discussed the effect of the transients to the BER. We also analyzed the influence of different transmission line parameters on the channel gain. The results show that the TL parameters have a similar influence on the channel for both transient and non-transient models.